WL-TR-91-2139

EVALUATION OF DOPED POLYETHYLENE OXIDE AS SOLID ELECTROLYTE FOR POLYMER BATTERIES

A.K. Sircar, P.T. Weissman, and B. Kumar

University of Dayton Research Institute
300 College Park Avenue
Dayton, Ohio 45469-0170

February 1992

Final Report for Period August 1991 - October 1991

AERO PROPULSION & POWER DIRECTORATE
WRIGHT LABORATORY
AIR FORCE SYSTEMS COMMAND
WRIGHT-PATTERSON AIR FORCE BASE, OHIO 45433-6563

NOTICE

When Government drawings, specifications, or other data are used for any purpose other than in connection with a definitely Government-related procurement, the United States Government incurs no responsibility or any obligation whatsoever. The fact that the government may have formulated or in any way supplied the said drawings, specifications, or other data, is not to be regarded by implication, or otherwise in any manner constructed, as licensing the holder, or any other person or corporation; or as conveying any rights or permission to manufacture, use, or sell any patented invention that may in any way be related thereto.

This report is releasable to the National Technical Information Service (NTIS). At NTIS, it will be available to the general public, including foreign nations.

This technical report has been reviewed and is approved for publication.

LAWRENCE G. SCANLON, JR.
Task Manager

RICHARD A. MARSH
Technical Area Manager
Batteries and Fuel Cells
Power Technology Branch

FOR THE COMMANDER

MICHAEL D. BRAYDICH, Lt.Col, USAF
Deputy Director
Aerospace Power Division
Aero Propulsion & Power Directorate

If your address has changed, if you wish to be removed from our mailing list, or if the addressee is no longer employed by your organization, please notify WL-POOS-2, WPAFB, OH 45433-6563 to help us maintain a current mailing list.

Copies of this report should not be returned unless return is required by security considerations, contractual obligations, or notice on a specific document.

UNCLASSIFIED
SECURITY CLASSIFICATION OF THIS PAGE

REPORT DOCUMENTATION PAGE

Form Approved
OMB No. 0704-0188

1a. REPORT SECURITY CLASSIFICATION Unclassified	1b. RESTRICTIVE MARKINGS None
2a. SECURITY CLASSIFICATION AUTHORITY N/A	3. DISTRIBUTION/AVAILABILITY OF REPORT Approved for public release; distribution is unlimited.
2b. DECLASSIFICATION/DOWNGRADING SCHEDULE N/A	
4. PERFORMING ORGANIZATION REPORT NUMBER(S) UDR-TR-91-135	5. MONITORING ORGANIZATION REPORT NUMBER(S) WL-TR-91-2139
6a. NAME OF PERFORMING ORGANIZATION University of Dayton Research Institute 6b. OFFICE SYMBOL (If applicable)	7a. NAME OF MONITORING ORGANIZATION Wright Laboratory Aero Propulsion and Power Laboratory
6c. ADDRESS (City, State, and ZIP Code) 300 College Park Avenue Dayton, OH 45469-0170	7b. ADDRESS (City, State, and ZIP Code) Wright-Patterson AFB, OH 45433-6563
8a. NAME OF FUNDING/SPONSORING ORGANIZATION WL Aero Propulsion & Power Laboratory 8b. OFFICE SYMBOL (If applicable)	9. PROCUREMENT INSTRUMENT IDENTIFICATION NUMBER F33615-87-C-2714, Task No. 31
8c. ADDRESS (City, State, and ZIP Code) Wright-Patterson AFB, OH 45433-6563	10. SOURCE OF FUNDING NUMBERS PROGRAM ELEMENT NO. 61102F; PROJECT NO. 2303; TASK NO S4; WORK UNIT ACCESSION NO. 01

11. TITLE (Include Security Classification)
Evaluation of Doped Polyethylene Oxide as Solid Electrolyte for Polymer Batteries

12. PERSONAL AUTHOR(S)
A.K. Sircar, P.T. Weissman, and B. Kumar

13a. TYPE OF REPORT	13b. TIME COVERED	14. DATE OF REPORT (Year, Month, Day)	15. PAGE COUNT
Final	FROM 8/1/91 TO 10/31/91	1992 February	48

16. SUPPLEMENTARY NOTATION
N/A

17. COSATI CODES			18. SUBJECT TERMS (Continue on reverse if necessary and identify by block number)
FIELD	GROUP	SUB-GROUP	battery, ionic conductivity, polymers, PEO, electrolytes, and characterization
10	02		
21	03		

19. ABSTRACT (Continue on reverse if necessary and identify by block number)

This report presents results of an investigation on preparation and characterization of polyethylene oxide (PEO) and lithium tetrafluoroborate ($LiBF_4$) complexes for application as solid electrolytes in polymer batteries. AC conductivity and permittivity (dielectric constant) as a function of frequency, temperature, and concentration of lithium tetrafluoroborate ($LiBF_4$) in polyethylene oxide (PEO) films were measured with a TA Instruments DEA 2970, Dielectric Analyzer. Differential Scanning Calorimetry (DSC) was used to trace changes of the morphology of the polymeric medium. Thermogravimetry (TG)/derivative thermogravimetry (DTG) were used to follow the decomposition of components and define the maximum temperature limits for these measurements. Infrared Spectroscopy monitored structural evolution as the O:Li ratio in the polymer complex was varied. Thin films of a complex (O:Li = 8) were used to assemble Li/Polymer/Li Cell for electrochemical characterization. (Continued on other side)

20. DISTRIBUTION/AVAILABILITY OF ABSTRACT	21. ABSTRACT SECURITY CLASSIFICATION
☒ UNCLASSIFIED/UNLIMITED ☐ SAME AS RPT. ☐ DTIC USERS	Unclassified

22a NAME OF RESPONSIBLE INDIVIDUAL	22b. TELEPHONE (Include Area Code)	22c. OFFICE SYMBOL
R.A. Marsh	513-255-7770	WL/POOS-2

DD Form 1473, JUN 86 *Previous editions are obsolete.* SECURITY CLASSIFICATION OF THIS PAGE

UNCLASSIFIED

19. ABSTRACT (Continued)

The study showed that the relationship of dopant concentration to electrical properties is rather complex. Degree of ion-pairing, dissociation of ions on dilution, changes in the morphology of the polymeric medium, and variations in viscosity and its consequence on ion mobility were considered to explain the data. An optimum in room conductivity occurred in a complex with O:Li ratio of 8.

TABLE OF CONTENTS

LIST OF FIGURES

LIST OF FIGURES (Continued)

LIST OF TABLES

ACKNOWLEDGEMENTS

The authors would like to thank Jonathon A. Foreman of TA Instruments, Inc. for consultations during the course of this investigation and Dr. Larry Scanlon of the Battery Laboratory for helpful criticism. Thanks are also due to Ruth Rodak for editorial comments and to Jeanne Miller for secretarial help. This work was financed by the Aeopropulsion and Power Directorate of the Wright Patterson Air Force Base under Contract No. F33615-90-C-2036.

SECTION 1
INTRODUCTION

Solid polymer electrolytes are gaining increasing importance in solid-state electrochemistry in view of their potential applications in high energy density batteries and sensors. In recent years, a great deal of interest and activity has emerged to develop polymers with high electrical conductivity (~10^{-2} S cm^{-1} at room temperature). A class of polymer, generally known as a polymer-salt complex that consists of a polymer and alkali salts has been the focal point of intense research efforts. The polymers used in this class of electrolytes, by virtue of their molecular structure, allow significant mobility of alkali ions. This gives rise to a material that has high ionic conductivity and is useful for intended applications. Despite significant progress in the materials development effort, a few major issues such as interfacial (electrode-electrolyte) chemistry, stability of electrolyte, cyclability, and high room temperature conductivity are yet to be understood and resolved.

The purpose of this investigation was to formulate and characterize polyethylene oxide (PEO) and lithium tetrafluoroborate ($LiBF_4$) complexes with a view to develop a material with high ionic conductivity that may be useful as solid electrolyte. This report will present results of characterization of the synthesized material to delineate electrical, thermal, and structural properties.

SECTION 2
EXPERIMENTAL

Material Preparation - Polyox N750, supplied by Union Carbide, was used for PEO. The number average molecular weight reported by the manufacturer is 300,000. Manufacturer's literature shows that it contains ~3% fused silica. Melting point (Tm) of the sample was 68.5°C, as determined by Differential Scanning Calorimetry (DSC) peak temperature (T_p). $LiBF_4$ was chosen as the dopant because of its low lattice energy.

Films containing the dopant were cast in a Teflon mold from solutions containing the components in the desired ratio in acetonitrile and dried under partial vacuum at room temperature for 24 hours. These were used for DSC and TG experiments. For conductivity and dielectric measurements, films were cast into the electrode itself to avoid contact resistance. The technique provided reproducible data. The films were very hygroscopic and were stored in a vacuum dessicator until needed for the measurements. Once the films were exposed to open atmosphere, they had to be kept in vacuum dessicator for 24 hours before the enclosed films were relatively free of moisture.

Dielectric Measurements - The dielectric analyzer DEA 2970 by TA Instruments DEA 2970 measures capacitance and conductance of a material as a function of time, temperature, and frequency[1]. Four major properties are analyzed during dielectric analysis: e' = permittivity (also called dielectric constant); e" = loss factor; Tan δ = dissipation factor (e"/e'); and σ^{-1} = ionic conductivity (S cm^{-1}). In simple terms, e' represents the amount of alignment of the dipoles to the electric field. The loss factor, e", measures the amount of energy required to align the dipoles or move ions. Ionic conductivity is derived from loss factor e" as follows:

$$\sigma = e'' \omega e_0 \qquad (1)$$

where: σ = ionic conductivity,
ω = angular frequency ($2\pi f$),
f = frequency (Hz), and
e_0 = absolute permittivity of the free space (8.85×10^{-12} F/m).

The TA Instruments DEA 2970 is capable of operating between -150 and 500°C with the single-surface electrode used. It should have an ionic conductivity range from 10^{-17} to 10^{-2} mhs/cm (per the TA Instrument brochure), at a frequency range of 0.003 Hz to 100 KHz. Usually, conductivity values in the range of 10^{-3} to 10^{-4} S cm^{-1}

at 80°C-100°C, falling to 10^{-6} to 10^{-8} S cm^{-1} at room temperature, are common for polymer electrolytes in the literature [2]. DEA 2970 was expected to be capable of measurements at these ranges [1]. It is also capable of scanning 28 different frequencies in one experiment and can operate in a programmed heating or cooling mode. The electrode assembly is confined in a glass dome (which offers protection from humid air) and can be operated under vacuum or in the presence of a purge gas. A heating rate of 1°C/min under nitrogen purge was used for these experiments. A single-surface electrode was used to avoid complications with the parallel electrode due to the change in thickness during programmed heating to high temperatures (up to 200°C).

DSC Measurements - Melting temperature and relative crystallinity (as measured by enthalpy) of doped and undoped PEO were determined by TA Instruments 2910 DSC at a heating rate of 10°C/min under nitrogen purge. Pure indium was used for temperature and enthalpy calibration. The sample was weighed and then returned to the vacuum dessicator for a minimum of four hours before the DSC experiment to remove the moisture absorbed during weighing. There were also differences in the first and second run due to differences in the prehistory of the samples. The parameters measured from the DSC endotherms are enthalpy (ΔH_m), temperature of origin of the endotherm (T_o), peak temperature (T_p), and temperature of the end of the endotherm (T_e).

Thermogravimetry - TA Instruments 2950 Thermogravimetric Analyzer TGA was calibrated with indium wire for temperature measurements. Samples were run at 10°C/min under nitrogen.

Infrared Spectroscopy - Infrared (IR) vibrational spectra were obtained using a Nicolet SX60 FTIR spectrometer. The polymer specimen was dissolved in acetonitrile. A thin film suitable for IR transmission measurement was prepared by placing three to four drops of the polymer solution on an AgCl crystal. The solvent was allowed to evaporate in a hood. The specimen was kept in a vacuum atmosphere for 12 hours, then transferred to a dry box for an additional 24 hours before spectral measurement.

Impedance Spectroscopy - The AC impedance measurement of the Li/Polymer/Li cell was conducted using EG&G, Princeton Applied Research Model 368, AC impedance meter.

Fabrication of Li/Polymer/Li Cells - Several Li/Polymer/Li cells were assembled using films of an electrolyte with an O:Li ratio of eight. Copper was used as current collectors. The fabricated cells were rectangular with an area of 6.5 cm^2.

SECTION 3
RESULTS AND DISCUSSION

Basic Considerations:

The usefulness of PEO as a polymer electrolyte is based on the great flexibility of the PEO backbone. The polymer chain can take conformations that will favor its complexations with alkali metal salts either by hydrogen bonding or by ion-dipole interactions with the oxygen electron pair[3,4]. A neutral polar polymer, $(AB)_n$, complexed with a mono-univalent metal salt MX (where M is an alkali metal and X is a fairly "soft"[5] anion or an anion with low lattice energy (I^-, SCN^-, $CF_3SO_3^-$, ClO_4, CF_3COO^-, $H_2PO_4^-$, BF_4^-, etc.) may be schematically represented as follows:

$$(AB)_n + MX \rightarrow (AB)_n \cdot MX. \qquad (2)$$

The -AB- polymer subunit, in the case of PEO, contains a Lewis base (O:) which interacts energetically in the "solvation" or "complexation" of the cation M^+.

Several criteria for forming of polymer electrolytes via equation (2) have been outlined[6,7] and described by Ratner[8] in a review article.

(a) The salt should have relatively small lattice energy; this is aided by choosing anion X^- to be soft[5], large, and the conjugate base of a strong acid.

(b) The polymer should have low cohesive energy density. This should be favored by low glass transition temperature, Tg.

(c) The base group, B, of the polymer repeating unit, (AB), should have good complexing properties. Normally, this requires a high concentration of polar groups.

(d) The polymer chain should be flexible (low Tg), both to ensure effective solvation of cations and to provide favorable solvation entropy.

It has been demonstrated[6,7,9,10] that PEO will effectively form complexes only if the lattice energy of MX in equation (1) is below a certain threshold value (roughly 850 KJ/mole). From considerations of lattice energy as well as the charge density and basicity of the ion, it was recommended[11,12] that the most suitable anions for polymer

electrolytes should be BF_4^- or ClO_4^-. Therefore, $LiBF_4$ was selected as a dopant for this study.

DSC Studies - To understand the conductivity behavior of the PEO/$LiBF_4$ system, it is necessary to first understand its phase behavior. The phase behavior of polymer electrolytes is rather cumbersome. Two or more phases (e.g., crystalline polymer, amorphous polymer, crystalline complex, amorphous complex, and crystalline salt) may coexist with one another. For PEO-based electrolytes, three phases have been observed and described: (1) a crytalline phase, generally spherulitic in nature, composed of PEO-MX (EO units/[M] = n) crystalline complex or of pure PEO; an "intracrystalline" phase, and (3) an "intercrystalline" phase. The last two phases are both amorphous[13]. Moreover, the ratio of different phases depends on PEO:MX ratio, time, temperature, etc. Fauteux[13] observed that the "intracrystalline" phase predominates at low temperature. The "intercrystalline" phase predominates at temperatures higher than the melting temperature of pure PEO or at the eutectic and is in thermodynamic equilibrium with the PEO-salt crystalline complex. The determination of phase diagrams for these systems is complicated by the kinetics of crystallization, molecular weight distribution of the polymer, and the lack of complete crystallization of most polymer systems[13]. Despite these complications, different techniques including DSC[14-17], X-ray diffraction[18,19], optical microscopy[20], and nuclear magnetic resonance (NMR)[21,22] have been used to determine the phase diagrams and formulas of polymer-salt complexes with variable success. A recent study [23] reports these diagrams of PEO:$LiBF_4$ and PEO:$LiCF_3SO_3$ systems with combined x-ray diffraction and DSC.

Table 1 and Figures 1 and 2 show the results of DSC experiments of the PEO/$LiBF_4$ samples of varying salt concentration. Three different stages are observed as the salt concentration progressively increases from pure PEO to pure lithium tetrafluoroborate. It may be observed that PEO crystallinity is affected even at an O:Li ratio of 9:1. Literature data[12] indicate that PEO crytallinity is affected at O:Li concentrations as low as 50:1.

As O:Li ratio decreases to 6:1, another high-temperature crystalline complex evolves. This complex gets more and more defined (symmetrical) and grows in enthalpy as salt concentration increases beyond 6:1. Also, T_p increases to a maximum at 3:1 (O:Li). As salt concentration increases further, T_p decreases. An explanation of these curves is provided in the following paragraphs.

TABLE 1

DSC DATA FOR POLYETHYLENE OXIDE
DOPED WITH LITHIUM TETRAFLUOROBORATE

Oxygen:Li	Weight Fraction	T_o (°C)	T_p (°C)	T_e (°C)	ΔH_m (J/g)	Comments
1:0	0	51.1	68.5	77.0	142	Virgin polymer
9:1	0.191	12.3	54.4	65	62.6	Low temp. complex with PEO
8:1	0.210	10.3	58.9	68.3	79.9	"
7:1	0.233	28.1	60.0	70.5	41.6	"
6:1	0.262	35.3	57.4	63.0	24.3	Low temp. complex
		80.4	108.6	121	7.2	High temp. complex
5:1	0.299	33.8	58.6	66.2	31.7	Low temp. complex
		97.4	129.5	138.1	21.8	High temp. complex
4:1	0.348	17.9	55.3	70.1	24.4	First heat
		99.0	143.3	156.3	32.5	First heat
		45.4	56.9	62.8	5.4	Second heat
		91.4	139.4	150.3	38.9	Second heat
3:1	0.415	32.2	75.2	118.8	39.0	Low temp. complex
		124.6	151.7	159.9	66.9	High temp. complex
2:1	0.516	70.1	93.6	100.4	32.6	Broad low temp. complex
		118.8	144.4	151.8	45.1	High temp. complex
1:1	0.681	40.2	97.8	113.9	157.1	A sharp peak ending in another broad peak
		113.9	136.5	194.4	67.2	
0:1	1.0	84.3	115.8	122.7	282.8	Double peaks
		122.7	131.7	179.4	179.1	"

Table 1 summarizes the data (T_o, T_p, T_e, and ΔH_m) for the DSC experiments. A sharp drop in both T_o and ΔH_m is observed at the first stage. Also, the endotherms for low lithium concentrations up to O:Li = 7:1 show broad, skewed patterns indicating a broad distribution of crystallite size. Lower T_p, as compared to PEO, indicates smaller crystallite sizes. Lower ΔH_m shows a lower degree of crystallinity. T_p varies from 55 to 60°C at these compositions. A rapid drop of crystallinity, as measured by ΔH_m vs. $LiBF_4$ concentration is observed as O:Li decreases to 6:1. This is shown in Figure 3, curve A. Enthalpies (ΔH_m) of lower and higher temperature endotherms for complexes depicting two peaks are plotted in Figure 3 curves B and C, respectively. Enthalpies progressively increase after the minimum at 0.3 $LiBF_4$.

Also, morphology of these complexes depends on the prehistory of the sample as will be observed by comparing first and second runs of the same sample (O:Li = 4:1) in Figure 2 curves A and A'. This is contrary to the observation of Lee and Wright[24], who observed the same melting temperature for the annealed and unannealed samples (PEO-NaSCN), although they observed differences in lamellar thickness by electron micrography.

At PEO:$LiBF_4$ = 3:1 (Figure 2B) a very broad low temperature endotherm and a very sharp high temperature endotherm with a peak at 152°C are observed. The symmetry and sharpness of the latter endotherm indicate highly ordered, narrowly distributed crystallites. Literature data as well as maximum T_p values (Table 2) indicate that this is due to the formation of a eutectic composition. It is interesting that the T_p of the eutectic composition is higher than that of either component.

At intermediate compositions (O:Li = 6 to 3), the crystallites are believed to be a mixture of high- and low-temperature complexes. At compositions higher than 3:1, unreacted lithium salt may remains[23]. The similarity of the shape of the curves for PEO:$LiBF_4$ = 1:1 (Figure 2, curve D and $LiBF_4$) (Figure 2, curve E), although differing in temperature of transitions, lends support to this conclusion. Double peaks for $LiBF_4$ are due to subsequent decomposition after melting, as confirmed by the thermogravimetric (TG) curve in Figure 4. $LiBF_4$ shows two peaks; the lower temperature peak around 130°C correlates to the second DSC transition (Figure 2, curve E) and corresponds to about one third the total weight of fluorine.

In Figure 5, the peak temperatures for the single and double endotherms are plotted. This provides an idea of the temperature dependence of the phases as the weight

TABLE 2

TRANSITION TEMPERATURES FOR DIFFERENT PEO-SALT SYSTEMS

	Phase II T_1 (°C)	Phase I T_2 (°C)	Salt (°C)	MW	Reference
PEO-NaI (n=4)	---	200	661	---	23
	50-60	---		4×10^6	24
	50-67	195		5×10^6	26
PEO-NaSCN (n=4)	---	170	287	---	23
	50-60	195		4×10^6	24
	50-67	195		5×10^6	26
PEO-KSCN (n=4)	---	170	173	---	23
	100-110	172		4×10^6	24
PEO-$LiBF_4$ (n=4)	~67	160		5×10^6	25
PEO-$LiCF_3SO_3$ (n=4)	~60	190	180	5×10^6	25
PEO-$LiBF_4$ (n=3)	75	152	111	3×10^5	This work
PEO-$LiBF_4$ (n=4)	54	144	111	3×10^5	This work

fraction of lithium increases. Curve A on the left represents the decrease of PEO crystallinity at a low lithium concentration as discussed before. Curve B is a plot of T_p for the lower temperature transitions of the endotherms that have double transitions, corresponding to Figure 3, curve B. This includes the inflection for 7:1 (O:Li) in Figure 1. Curves A and B seem to meet and give a minimum at the O:Li ratio of 5:1; this indicates an eutectic composition. Evidence for an eutectic is suggested by the sharp low-temperature DSC peak of 5:1 (O:Li) composition in Figure 1F as well as by the minimum in enthalpy versus weight fraction Li curves in Figure 3.

The T_p for the high-temperature endotherm shows a maximum at O:Li = 3:1. Other researchers[23-27] indicate an eutectic around this composition. The sharp, high-temperature endotherm at this composition (Figure 2B) with a peak at 152°C, supports this conclusion. Wright and coworkers[24-27] as well as Hibma [28] reported 4:1 (O:Li) as the eutectic composition for a PEO-$LiBF_4$ system with melting points at ~67°C and 160°C, for the lower and higher temperature endotherms, respectively. Zahurak, et al.[23] reports 3.5:1 as the eutectic composition. However, these films were prepared from methanol solution; acetonitrile was used for ours. Wright and coworkers[24-27] reported that the morphology of the films can differ by using different preparation methods. Also, the molecular weight of their PEO was much higher (5,000,000) than ours (300,000). These factors may explain the differences in eutectic composition as well as the melting point of the crystalline complex. The transition temperatures for the eutectic compositions at (n=4, 3, or 3.5) for other workers are shown in Table 2 along with our data for n=3 and n=4. Wright and coworkers tried to rationalize the two transitions by suggesting the existence of two crystalline phases (I and II). Phase I, melting at a higher temperature, was described to be apparently independent of the nature of either the cation or anion for NaI, NaSCN, and $LiCF_3SO_3$ salt in high molecular weight PEO-based electrolytes. The melting temperature of Phase II was reported to be approximately the same for all PEO-salt mixtures studied. The lower melting temperature of PEO-$LiBF_4$ (n=4) in Phase I was attributed to the difference in crystalline morphologies and the lower melting temperature of the pure salt. The DSC curves reported by Zahurak, et al. do not show the lower temperature transition around 55 - 75°C.

Fauteux[13] reviewed the phase relationship of the PEO-MX system, including the contributions by Weston and Steele[29,30], Sorensen and Jacobsen[15], and Berthier and coworkers[14,21,22] for the PEO-$LiCF_3SO_3$ system. The last workers used both

DSC and NMR techniques. The value of the reported eutectic composition (n) varied; it was reported as 4, 3.5, and 3. Robitaille and Fauteux[18,31] demonstrated the usefulness of a phase diagram for PEO-$LiCF_3SO_3$, developed from the data obtained by DSC, DTA, NMR, conductivity, microscopy, and modelling. This phase diagram shows the presence of an eutectic composition between n=50 and n=100, and of an intermediate compound of stoichiometry n=3. The presence of the eutectic was confirmed by optical microscopy observations for electrolytes containing low salt concentration. Fauteux[13] concedes that there is difficulty in comparing literature data since experimental differences exist among different studies. Nevertheless, it is generally agreed that more than one crystalline intermediate compound is formed, and that a eutectic reaction occurs between the PEO and one of the intermediate compounds.

Thermogravimetry - Figures 6 through 8 show the thermogravimetry (TG) data for virgin PEO, PEO:$LiBF_4$ (8:1), and PEO:$LiBF_4$ (5:1) films. The Virgin PEO decomposes with a single DTG peak at 400°C, leaving about two percent residue at 600°C. Two PEO-lithium compositions, on the other hand, show two additional lower temperature DTG peaks. The first peak, around 70°C, is believed to be due to entrapped solvent (acetonitrile) which boils at 81.6°C. The second peak, between 250 and 280°C, may be due to the decomposition of the $LiBF_4$-PEO composition. The peak temperatures in Figures 7 and 8 are different indicating different stability of the complexes. A higher peak temperature as compared to pure $LiBF_4$ (Figure 4) indicates higher stability of the complexed salt validating higher T_ps in Figure 5, curve C. For both compositions, decomposition of $LiBF_4$ starts much below 150°C, accounting for the second DSC transition of $LiBF_4$ (Figure 2E). A slight increase in weight at the low temperature, as observed in Figure 7, is evidently due to absorbtion of moisture during the experiment. As expected, the proportion of the residue increases as the $LiBF_4$ ratio increases.

Infrared Spectroscopy - Figures 9 through 14 show IR absorption spectra of $LiBF_4$, PEO:$LiBF_4$ complexes and virgin PEO in the 1900-280 cm^{-1} range. Figures 9 and 10 correspond to the spectra of $LiBF_4$ and virgin PEO, respectively. The $LiBF_4$ spectrum shows major vibration band around 1650, 1050, 640, and 550 cm^{-1}, whereas the virgin PEO spectrum shows vibration band in the neighborhood of 1450, 1340, 1100, 950 and 850 cm^{-1}. As the proportion of dopant increases, the increased degree of complexation is characterized by band shifts as well as by the formation of new absorption bands. For example, at the low dopant concentration (O:Li=10 or 8,

Figures 13 and 14), where DSC only shows decreased PEO crystallinity (Table 1, Figure 3A), the IR spectral features reveal dominance of vibrational bands of virgin PEO and lack of $LiBF_4$ vibrational features, as expected. However, a new absorption band around 995 cm^{-1} appears indicating some complexation. This is not indicated in DSC curves. Similar IR vibration bands were also observed by Papke et al. [32] for 4.5:1, PEO:$LiBF_4$ complex. The 995 cm^{-1} band was ascribed to very strong anion internal mode. Broadening of the 1100 cm^{-1} peak (C - O - C stretching)[32] with dopant concentration may also indicate lower crystallinity[33] and complexing with oxygen. As the dopant concentration increases further to the range where DSC shows double peaks (O:Li=6, Figure 12) some shift of the major PEO peak at 1100 cm^{-1} to lower wave number and splitting of the 1100 cm^{-1} peak occur, indicating development of crystallinity [33]. Finally, at the DSC eutectic composition (O:Li=3, Figure 11) some shifts of the existing peaks, development of new peaks (e.g., 860 cm^{-1}, 993 cm^{-1}, 1180 cm^{-1}) and omission of some minor peaks are observed. Splitting of the 1100 cm^{-1} band into two sharp bands (14) indicate further development of crystallinity[33], expected for a eutectic composition. The 860 cm^{-1} band was tentatively ascribed by Papke et al.[32] to a totally symmetric A_{1g} mode involving a metal-oxygen breathing motion. It was inferred that PEO chain wraps around the lithium cation.

The absorption spectra in the 3109-2578 cm^{-1} region for PEO, $LiBF_4$ and PEO:$LiBF_4$ complexes are shown in Figures 15 through 20. The PEO (Figure 15) exhibits a broad C - H stretching band with a peak aroung 2890 cm^{-1} and inflexions at 2950, 2860, and 2800 as well as small absorption bands at 2760 and 2695 cm^{-1}. $LiBF_4$ (Figure 16) shows a featureless spectrum, as would be expected for an inorganic compound in this region. At low dopeant concentrations (O:Li=8 or 10, Figures 19 and 20), the absorption spectra are very similar to PEO spectrum, with a new absorption peak (inflexion) around 2920 cm^{-1}. The latter is absent in PEO spectrum and becomes more defined as the dopant concentration increases with probably minor shift to lower wave number (Figure 18). Finally, at the DSC eutectic composition, the new absorption peak seems to split up into two well defined vibration bands at ~2925 and 2910 cm^{-1}.

The IR spectra presented in Figures 9 through 20 suggest that at low dopant concentration (O:Li=8 or 10) the PEO features prevail in the absorption spectra, whereas the features of PEO:$LiBF_4$ complex show up at higher concentrations. At still higher dopant concentration (e.g., O:Li=2 or 1, not included in IR study), free $LiBF_4$ (ion pair) remains, as was also indicated by DSC. Formation of ion pair was indicated by

Papke et al.[32] in the case of $LiNO_3$ as dopant. Two NO_3^- bands arising from nitrate ions in two distinct environments were inferred. Evidence for ion pair interactions has also been presented for the PEO.$NsBH_4$ and PEO.$NaBD_4$ complexes[34].

Conductivity Measurements - Figure 21 presents the DEA-generated ionic conductivity data for PEO at different frequencies and at temperatures from 20°C to 200°C. Note that curves at 1000 Hz and beyond converge at temperatures above 80°C. It is believed that at low frequencies electrode polarization gives rise to low conductivity. As the frequency increases, conductivity increases until it approaches a value close to DC conductivity. In this work, the conductivity at the maximum frequency (100 kHz) has been considered as the "apparent conductivity" of the sample.

Conductivity increases at low temperature (up to ~70°C) may be correlated to PEO melting. The temperature effect between ~70 and 110°C is small. The subsequent small decrease may be due to the desorption of moisture. A small weight loss, starting around 100°C is also observed in TG/DTG curve for Virgin PEO (Figure 6). Apparent conductivity of virgin PEO at room temperature agrees with the literature values[3,4].

In Figure 22, the apparent conductivity at 100 kHz is plotted versus different dopant concentrations (marked in the curve). Room temperature conductivity increases as dopant concentration decreases within the range presented, except for the highest dopant concentration (O:Li, 1:1). It will be shown later that at a lower concentration, specific for this system, conductivity increases as dopant concentration increases, as would be expected from the disruption of crystallinity with higher dopant concentration (Figure 3). MacCallum and Vincent[12] report that for $LiClO_4$ in PEO, conductivity increases at an O:Li ratio of over 50:1 until a maximum is reached at 8:1. Conductivity falls as the salt content is raised still further.

The conductivity rise in Figure 22 shows a sigmoidal curve with a break at around 45 to 50°C. The break may represent melting of the respective low temperature crystallites present. The 1:1 (O:Li) ratio shows a different curve than others, probably due to excess $LiBF_4$ in the system. The temperatures more or less correspond to DSC transitions for 1:1 (O:Li) in Figure 2,Curve D. All the curves (except virgin PEO) converge to a maximum conductivity point and then show no change of conductivity with temperature. This suggests that the maximum conductivity reached is the limit for the highest conductivity that can be measured with this instrument. Consultation with the manufacturer's representative confirms this view.

Conductivity curves in Figure 22 decrease as the salt concentration increases; the opposite is observed in with low concentration of lithium (Figure 23). When a dopant salt is introduced into the polymer matrix, conductivity increases rapidly due to an increased number of charge carriers despite the viscosity increase through the growing number of transient crosslinks. However, at large enough concentrations, the viscosity increases and the ion mobility decreases to such an extent that a maximum in conductivity versus salt concentration occurs. It has been suggested[35] that a conductivity drop at higher salt concentrations is due not only to reduced ion mobility but also to the formation of neutral ion pairs which decrease the number of charge carriers, and therefore, reduce conductivity. In polyethers, as in PEO, the low dielectric constant (ε~5) favors an extensive ion-ion interaction. Therefore, to optimize conductivity, a compromise between the number of charge carriers (i.e., salt concentration) and their mobility must be made. In Figures 22 and 23, this compromise seems to be achieved at an O:Li ratio of 8:1. This is in agreement with MacCallum and Vincent[12] as well as with Zahurak et al.[23].

It has been shown recently, in the case of polypropylene oxide (PPO), that salts have a tendency to precipitate out at elevated temperature. It has been observed[36-37] that the higher the melting point of the salt, the lower the salt precipitation temperature (implying a stronger ion-ion interaction) and the easier it is for the salt to precipitate out. From Table 2, $LiBF_4$ has a comparatively low melting point. Therefore, its precipitation temperature should be high. Unfortunately, it is not possible to locate this point from the curves in Figures 22 and 23 because of the limitation of the equipment mentioned above.

Figure 24 shows the effect of lithium concentration on conductivity. As may be observed, conductivity increases with ion concentration, reaches a maximum, and then decreases. The reversal point beyond 0.5 weight fraction may be due to precipitation of the salt out of the complex with the formation of neutral ion pairs. The initial rise is due to the availability of more charge carriers. The decline beyond the maximum may be related to a decrease in ion mobility due to an increase in viscosity, as mentioned earlier. Ionic conductivity is determined by the product of the number of carrier ions and their mobility. Higher temperatures should increase both the dissociation of ions and their mobility. This explains the occurrence of conductivity maximum at a higher concentration as the measurement temperature increases.

According to Ratner[8], the most definitive work on crystallinity in the (PEO·MX) electrolytes has been reported by Berthiers group in Grenoble[4,21,22,38]. These researchers used a combination of thermal measurements by DSC and NMR relaxation time and concluded "that many PEO·MX complexes are partly crystalline, that as temperature changes the crystallinity changes as regions melt and ions move among phases, that effective conduction occurs only in elastomeric phase, that both crystalline PEO and salt-rich crystalline complex in the bulk sample inhibit conductivity and that the overall conductivity behavior is fixed by several phenomena, not merely activated ion motion."[8] The above observations would explain much of the DSC and conductivity data presented.

Dielectric Constant Measurements - Figures 25 through 28 show the permittivity (dielectric constant) plots corresponding to conductivity data in Figures 21 through 24. Permittivity variations with the solid and molten PEO (Figure 25) show changes similar to those of Porter and Boyd.[39] Literature values[40] of the high frequency dielectric constant for room temperature (ε=5) and molten PEO (ε=8) agree with the data presented (Figure 13).

Permittivity at high frequenies at different $LiBF_4$ concentrations (Figures 26 through 28) generally corroborates the conductivity data at high frequency. As in conductivity, permittivity increases at low dopant concentration, then decreases as the concentration is increased beyond 8:1 (O:Li) (Figures 26 and 27). Increasing temperature (Figures 26 through 28) causes permittivity to increase to a maximum, then decrease thereafter. The concentration at which this decrease takes place increases with increasing temperature. The explanations for conductivity data hold true for the dielectric constant also. However, in the case of the dielectric constant, the data are still within the measurement limits of the instrument except for very high temperatures and concentrations (Figure 26); above 150°C for 3:1 (O:Li) and 170°C for 1:1 (O:Li). These temperatures are over the melting temperature of the eutectic (for 3:1) and the decomposition temperature of the precipitated lithium salt (1:1) and the data collected at this range have little practical significance..

Fabrication and Characterization of Li/Polymer/Li Cells - Efforts on synthesis and characterization of PEO:$LiBF_4$ complexes led to a material corresponding to an O:Li ratio of 8:1 having the highest room temperature conductivity. A batch of films of this material was made for fabricating Li/Polymer/Li cells. Several cells were fabricated for evaluation. The area of the cells was 6.5 cm^2 and copper was used as current collectors.

Initially copper and lithium foils were pressed together before assembling and fabricating the cells. The entire cell assembly operation was conducted in a dry box. After cells were fabricated, they were immediately encapsulated using an inert polymeric material. After the encapsulating polymer was cured, the cells were removed from the dry box for characterization.

The complex-plane impedance diagram of an Li/Polymer/Li cell is shown in Figure 29. As anticipated, the resistance of the cell is high, ~30 kΩ at room temperature. The impedance diagram is typical of a cell configuration employing non-blocking electrodes. The cell was also cycled using an initial current of 0.5 mA. The charge and discharge curves of the cycling experiment are shown in Figure 30. In general, the curves show an increase of current in the beginning for about 5 to 10 minutes, then a peak or constant value is attained. Finally, exponential decay occurs until the direction of current flow is reversed. In two instances, when the current reached the maximum set point (0.5 mA) a decrease in voltage was noted (Cycles 1 and 2). The cell functioned for three cycles, then failed in the beginning of the fourth. The failure occurred by a precipitous drop of voltage. This suggests that a short may have developed.

Data analysis indicated that the current density (~80 mA/cm^2) was excessive during the cycling. Recommended drain rates for state-of-the-art polymer cells are in the range of 10 to 20 mA/cm^2. Thus, it is not at all surprising that the cell failed after only three cycles. Future experiments will be designed to conduct this experiment at lower current densities.

SECTION 4
CONCLUSIONS

A wide compositional range of PEO:$LiBF_4$ Complexes with O:Li ratios varying from 1 through 41 were synthesized. Specimens in film form were prepared to characterize electrical, thermal and structural properties. Following are the specific conclusions of the investigation.

(I) A PEO:$LiBF_4$ complex corresponding to an O:Li ratio of 8:1 yields a material with the highest conductivity around room temperature.

(II) The DEA was found to be an useful technique to measure ionic conductivity and dielectric constant because of the speed at which a large amount of data may be collected. However, it does have a limitation with respect to the upper conductivity that it can measure ($\approx 10^{-3.5}$ S cm^{-1}).

(III) DSC and TG/DTG data provide approximate phase relations and, in most cases corroborate the DEA data. Three different stages are inferred as $LiBF_4$ concentration increases from pure PEO to pure $LiBF_4$.

(IV) At lower concentrations of $LiBF_4$, a solid solution type of structure resembling PEO-like spectrum is obtained in IR. This is in general conformity with DSC, conductivity, and dielectric constant data.

(V) Li/Polymer/Li cells were assembled using the complex with an O:Li ratio of 8:1. These cells exhibit high resistance at room temperature. A cell was cycled at a current density of 80 MA/cm^2. The cell failure occurred during the initial stages of the fourth cycle.

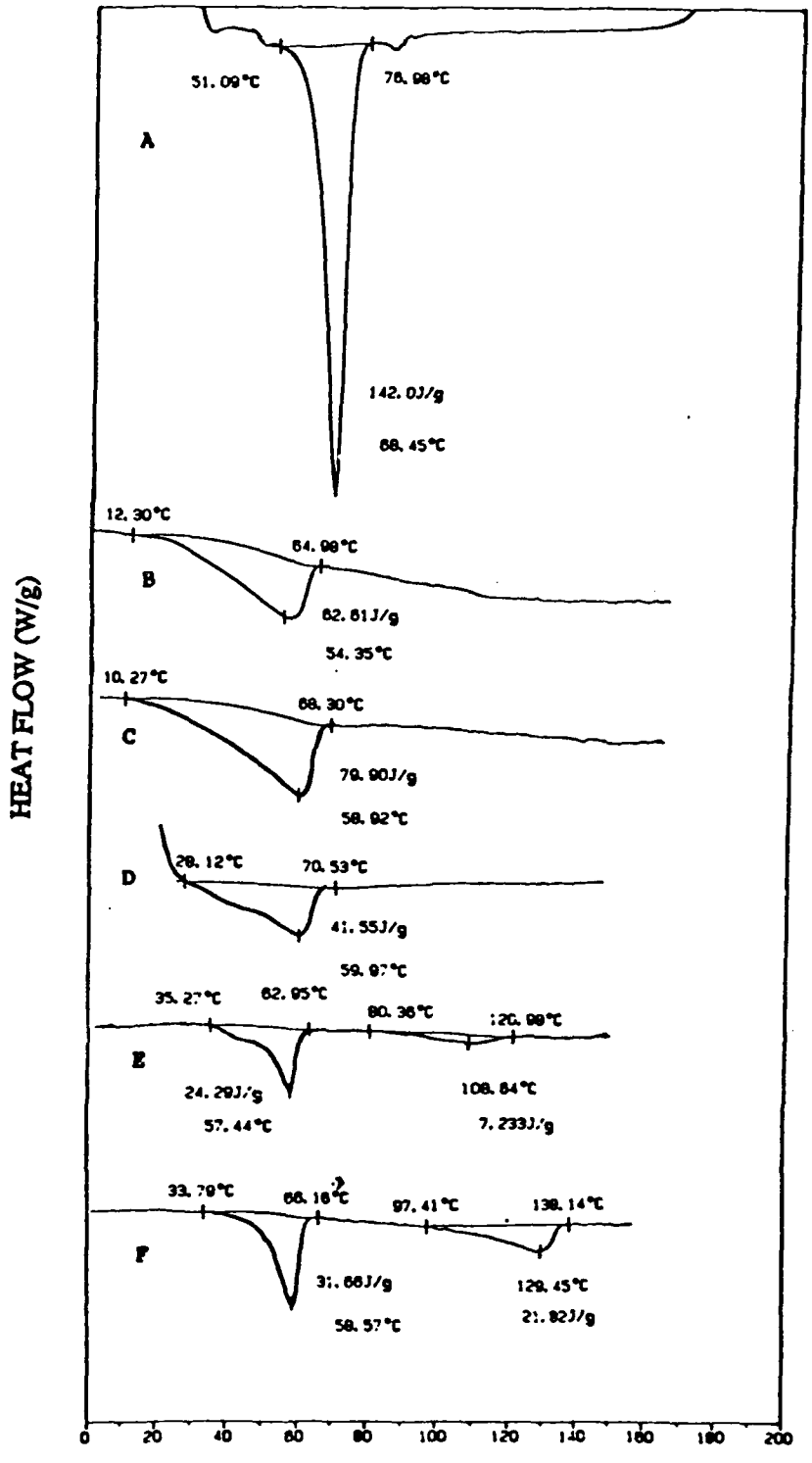

Figure 1. DSC Curves for PEO and PEO:$LiBF_4$ Compounds at Different Dopant Concentrations.

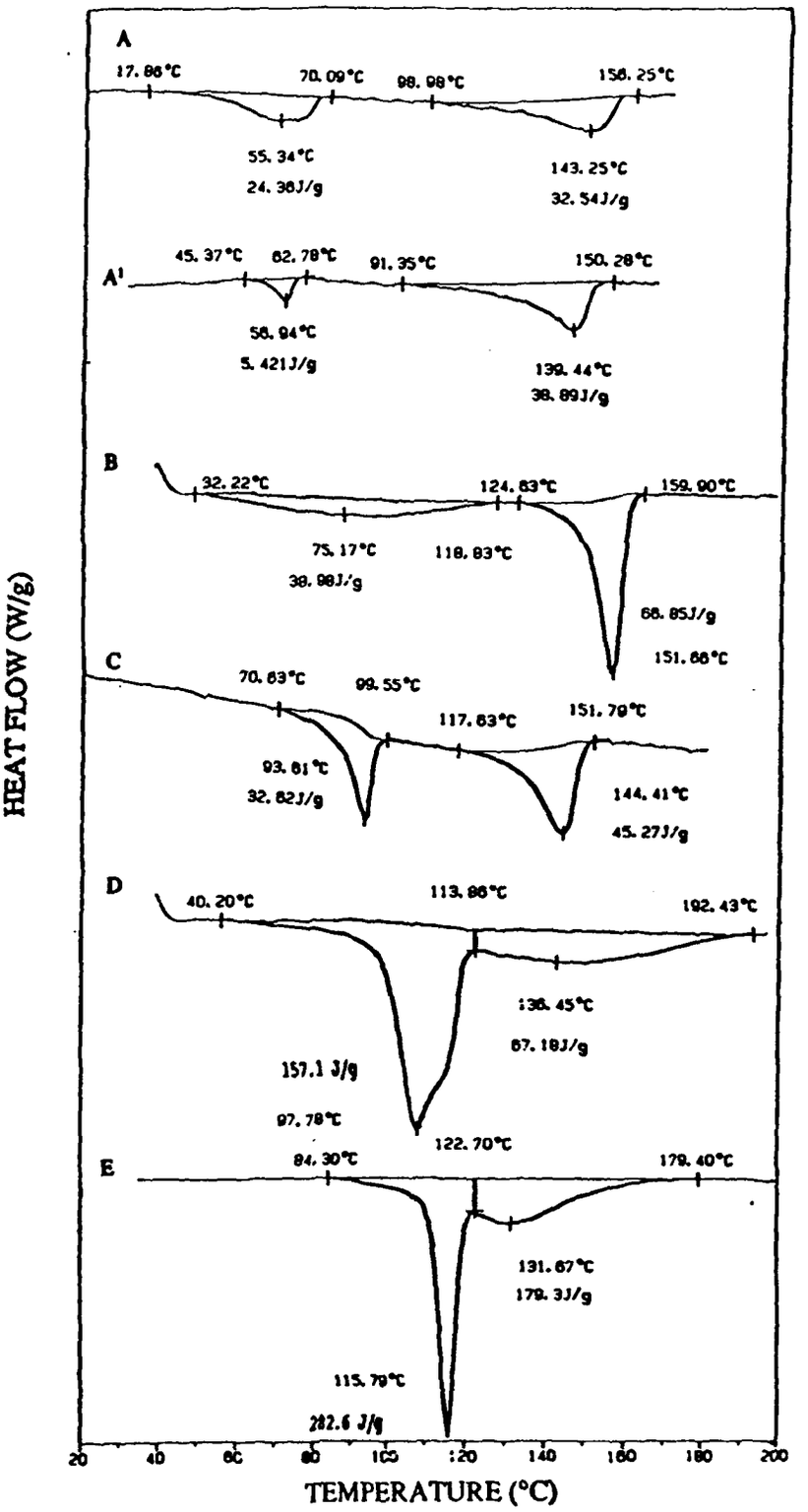

Figure 2. DSC Curves for $LiBF_4$ and PEO:$LiBF_4$ Complexes at Different Dopant Concentrations.

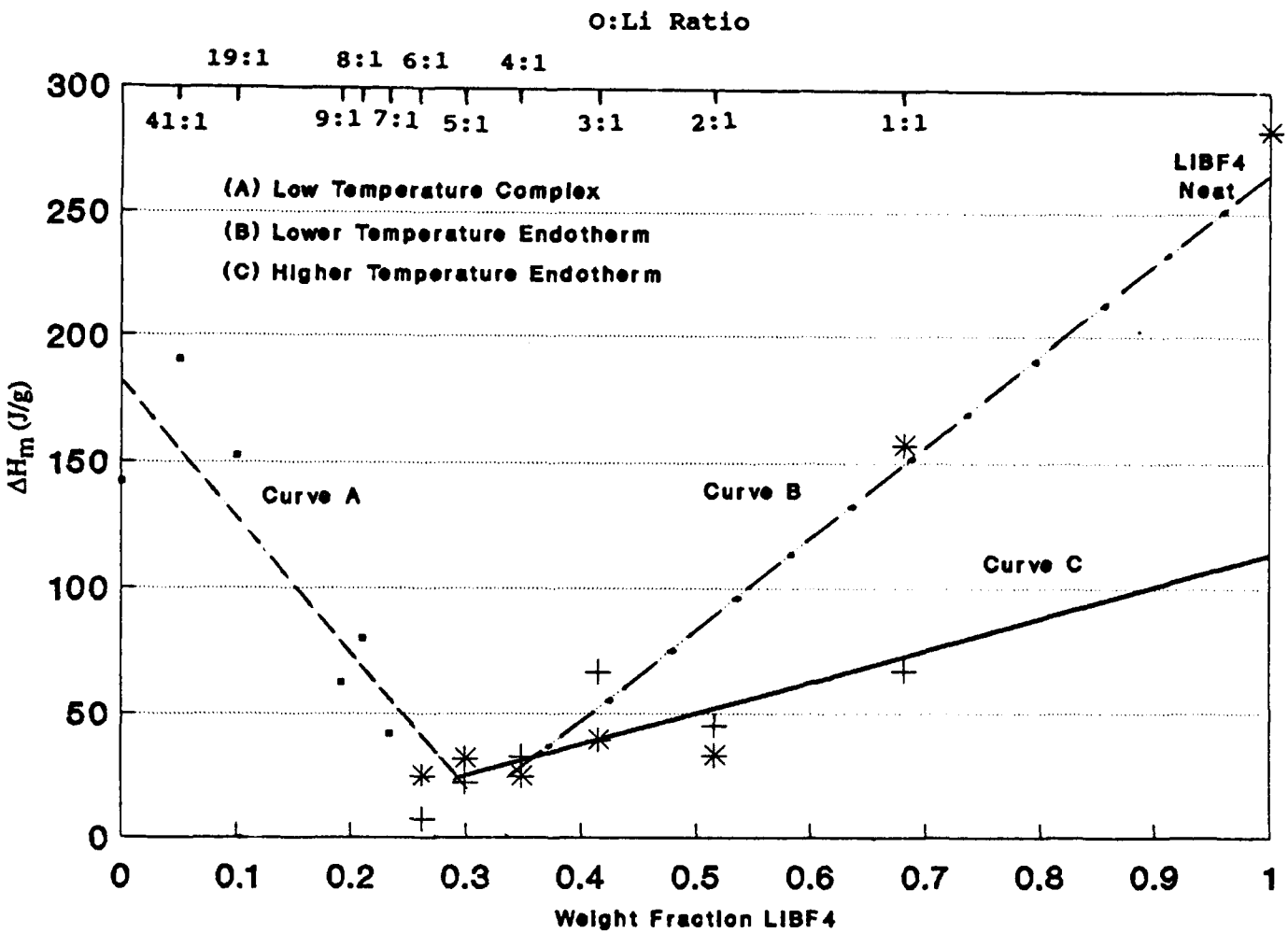

Figure 3. Crystallinity of PEO as a Function of Weight Fraction $LiBF_4$.

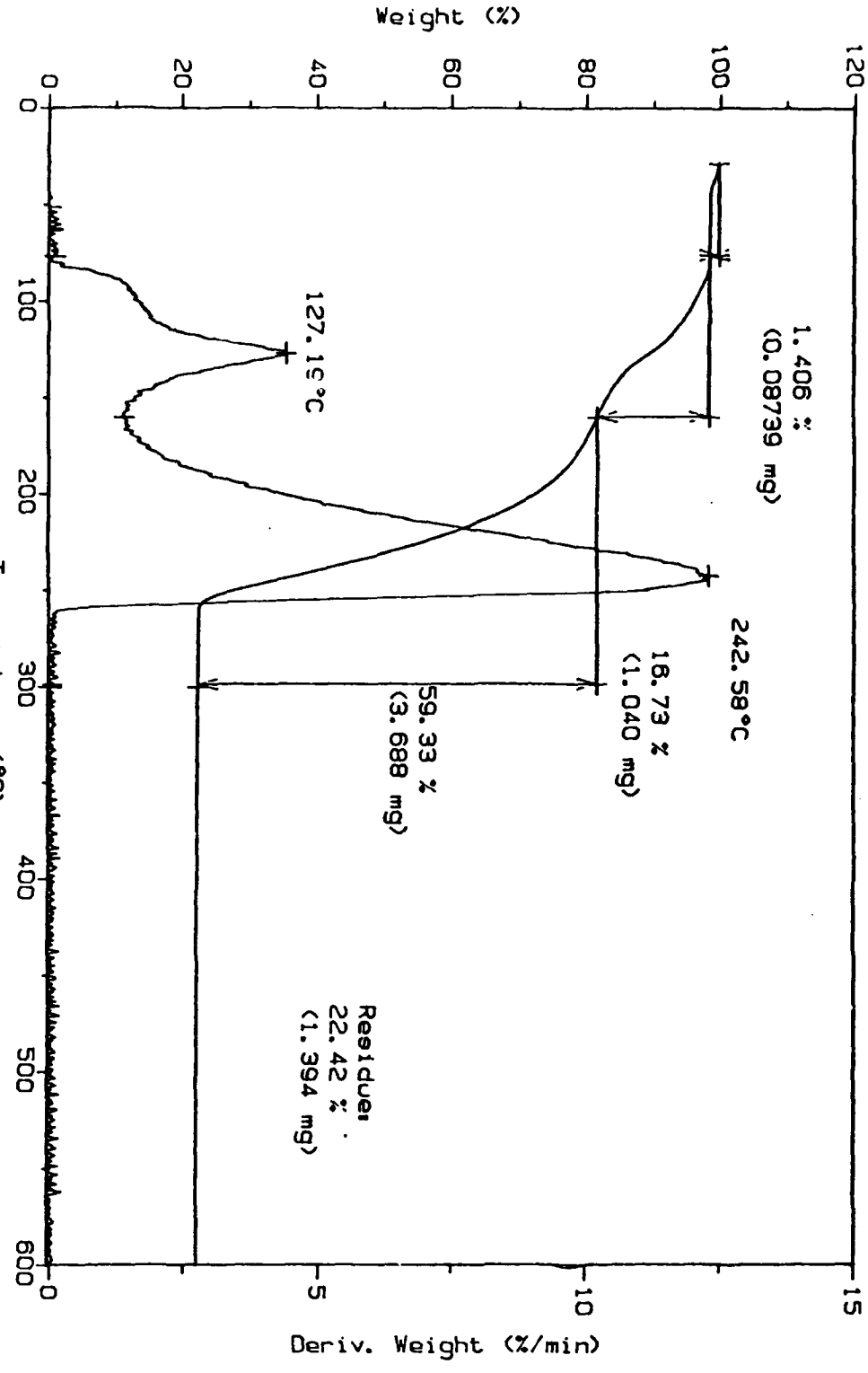

Figure 4. TG-DTG Curve for $LiBF_4$.

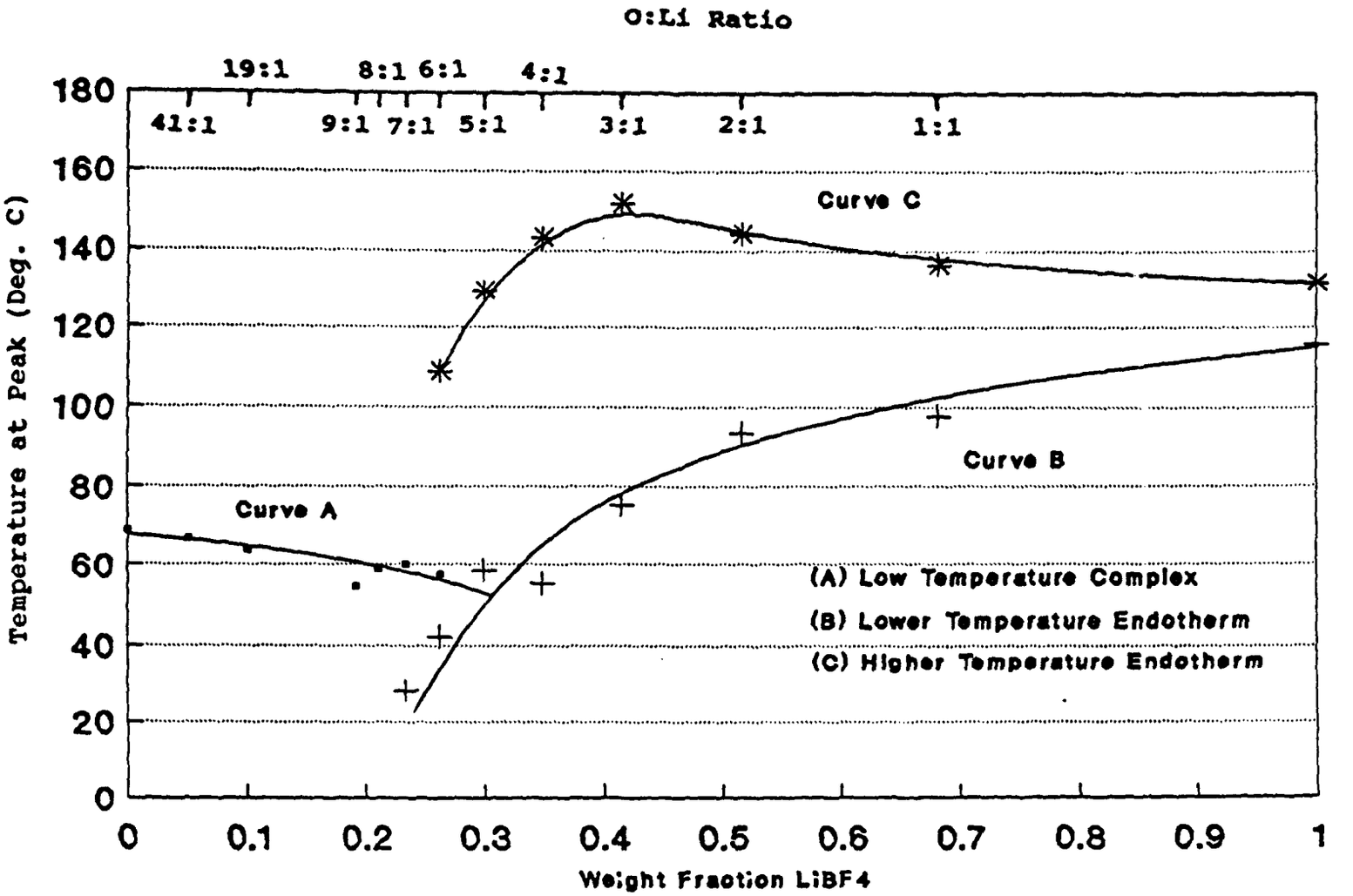

Figure 5. Peak Temperature of PEO:$LiBF_4$ Complexes as a Function of Weight Fraction of $LiBF_4$.

22

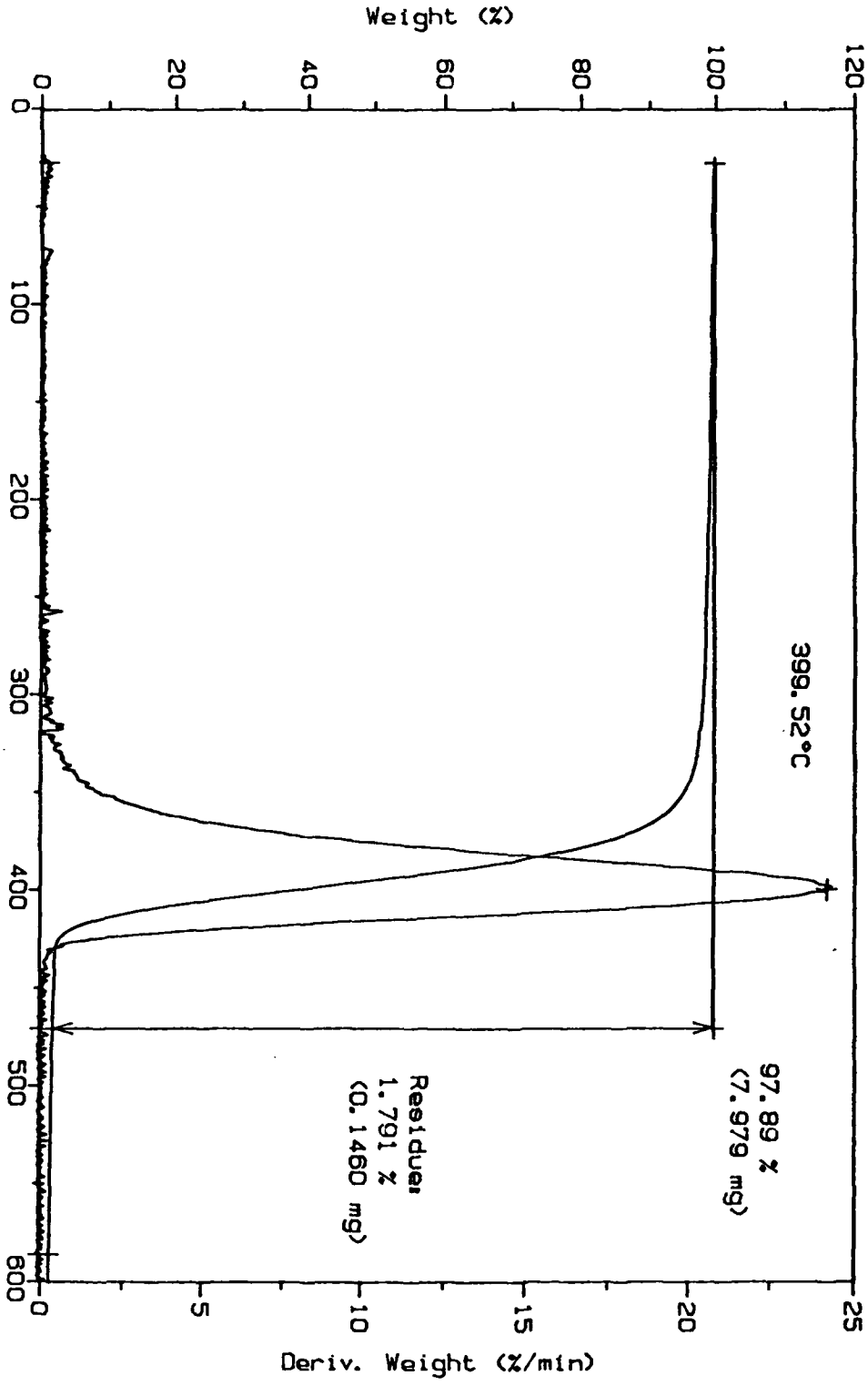

Figure 6. TG-DTG Curve for PEO.

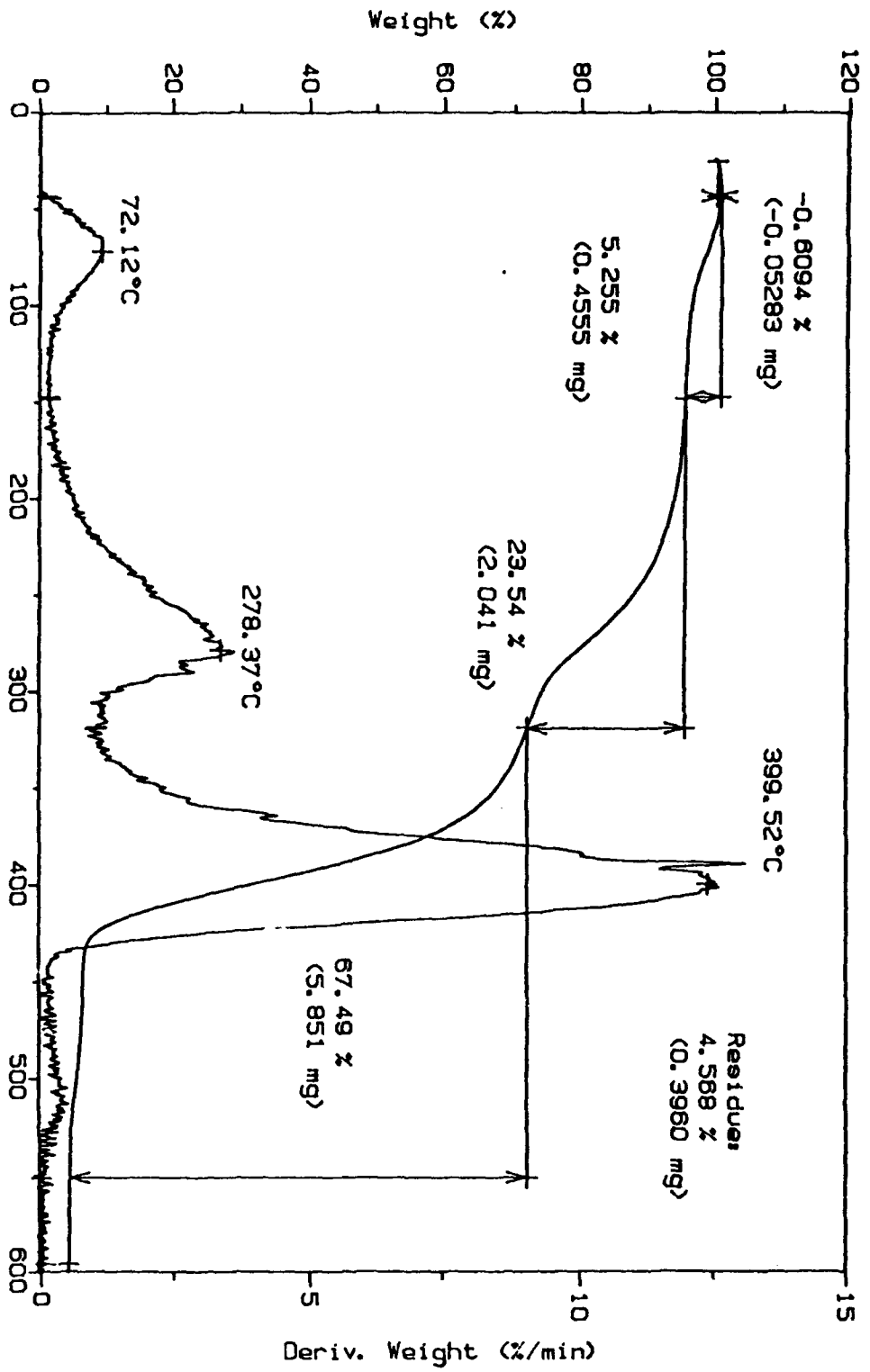

Figure 7. TG-DTG Curve for PEO:$LiBF_4$ (8:1).

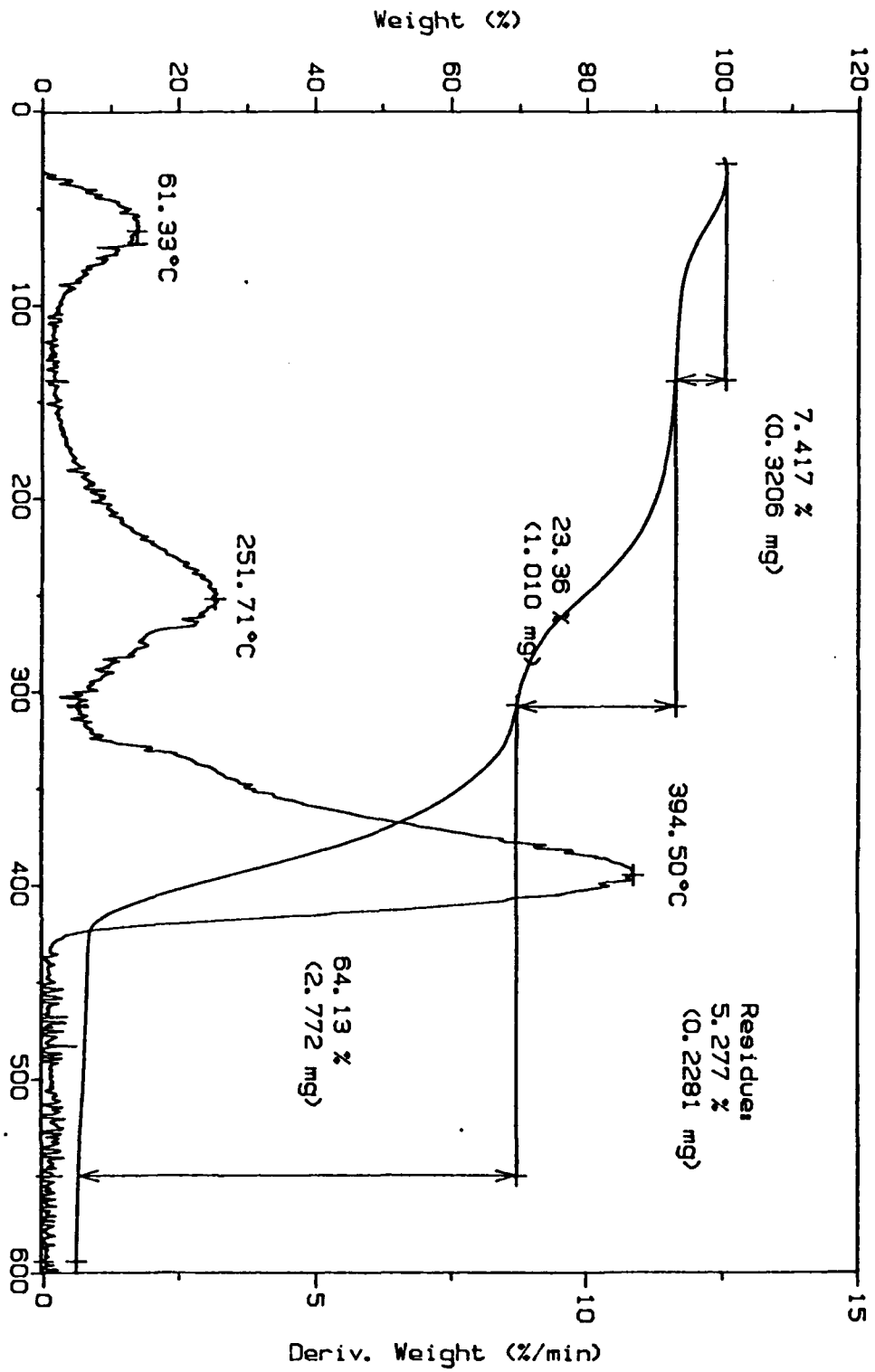

Figure 8. TG-DTG Curve for PEO:LiBF$_4$ (5:1).

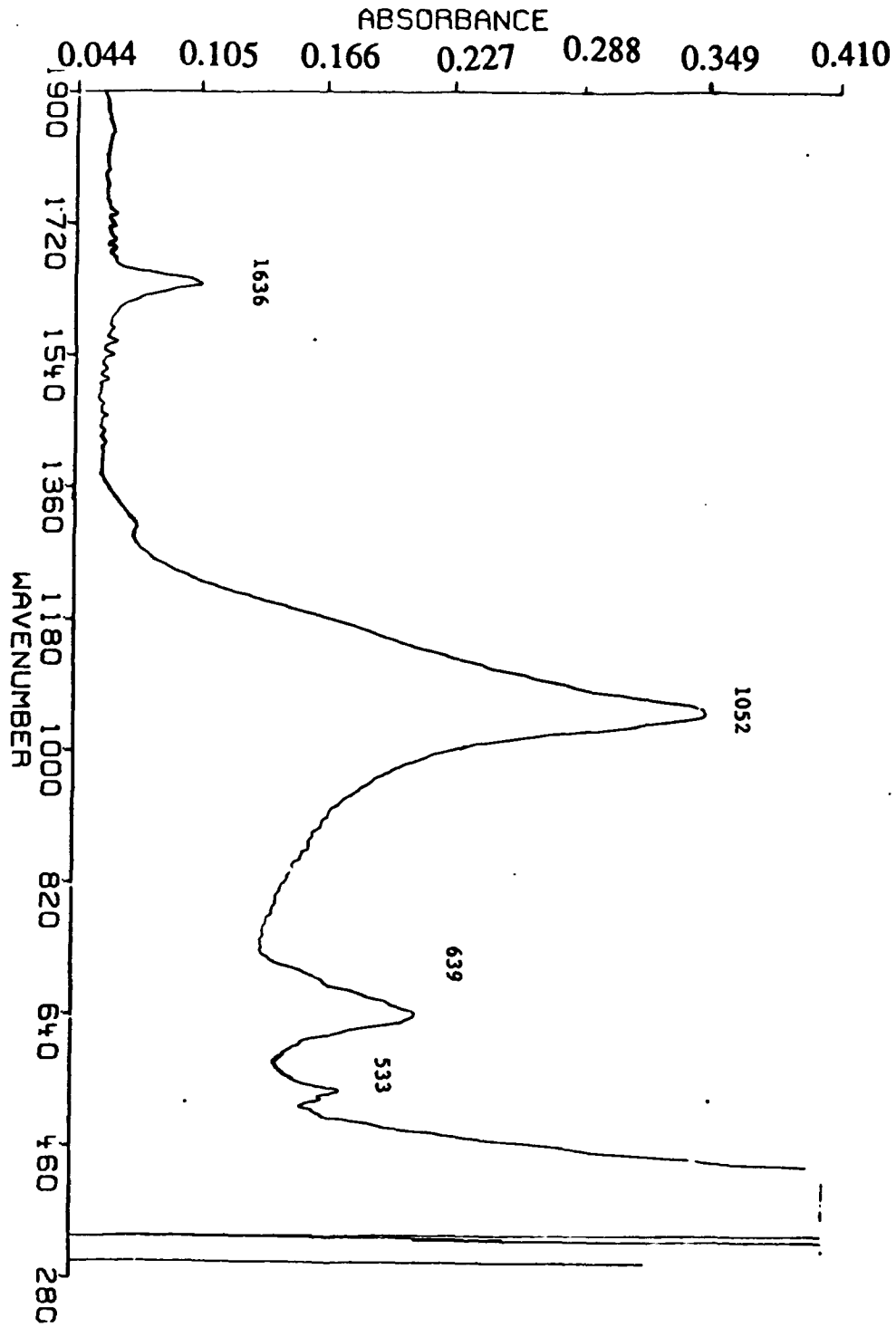

Figure 9. Absorbance Spectrum of $LiBF_4$ in 1900-280 cm^{-1} Region.

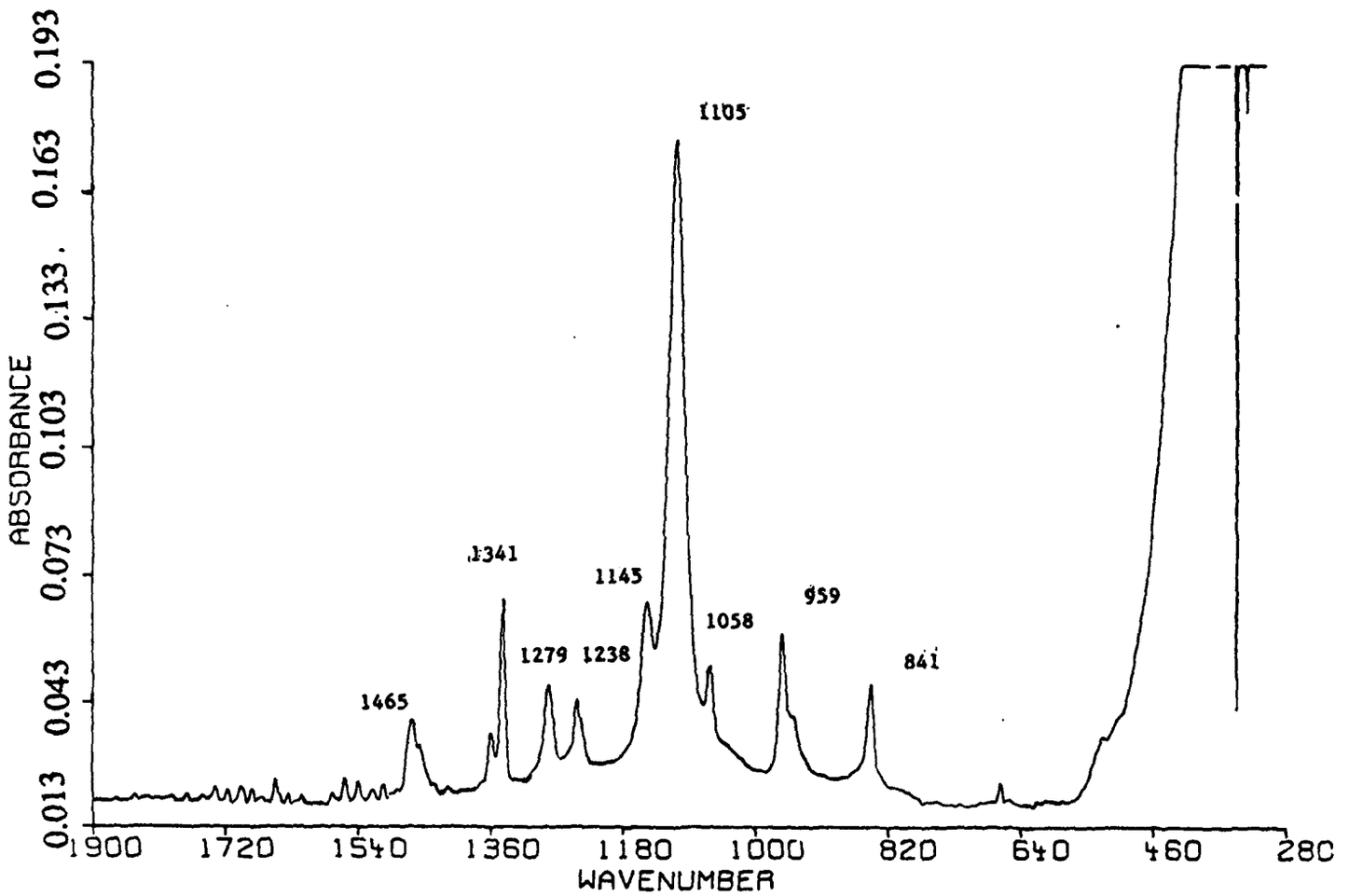

Figure 10. Absorbance Spectrum of Virgin PEO in 1900-280 cm^{-1} Region.

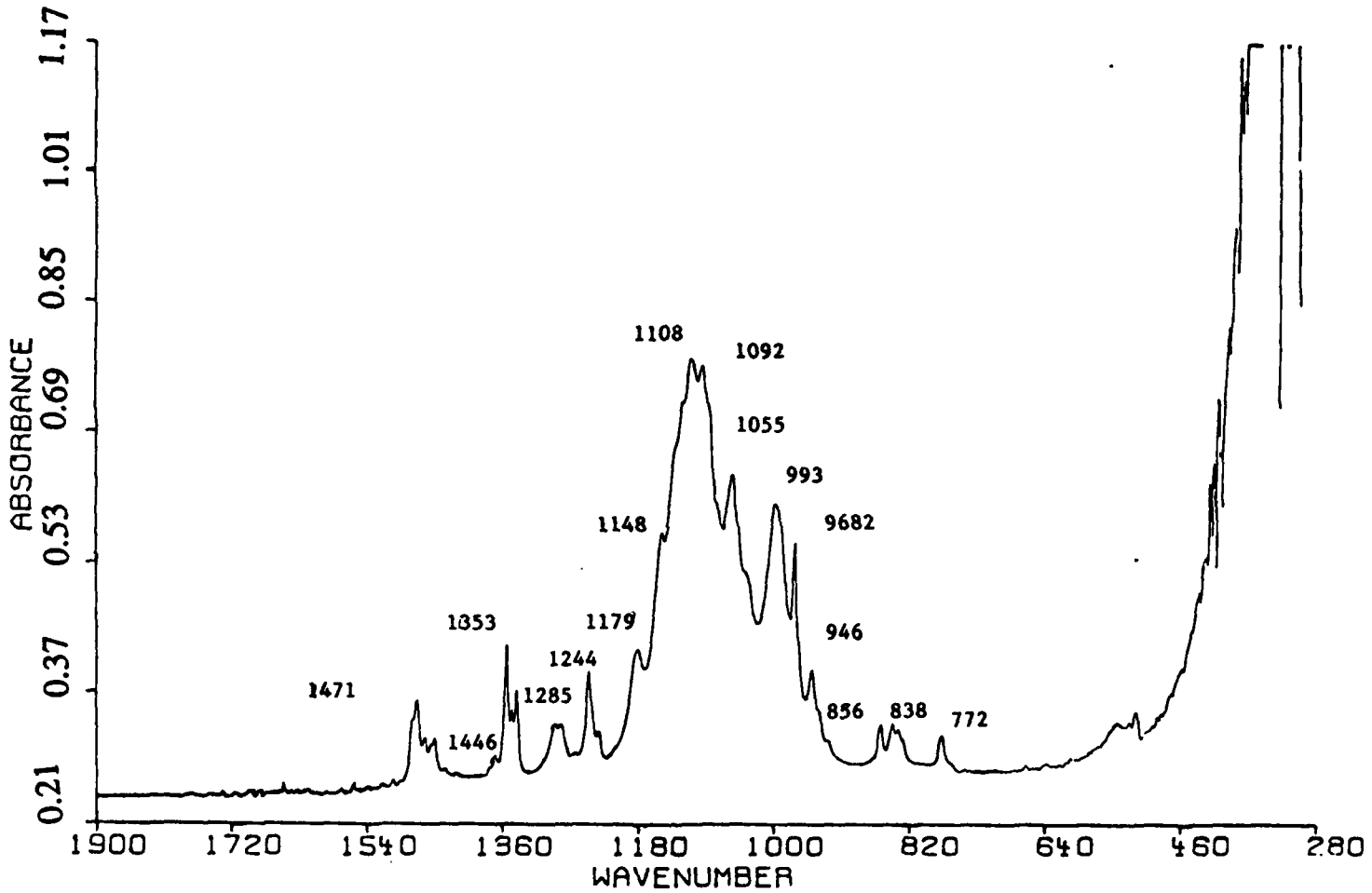

Figure 11. Absorption Spectrum of PEO:$LiBF_4$ Complex (O:Li = 3:1) in 1900-280 cm^{-1} Region.

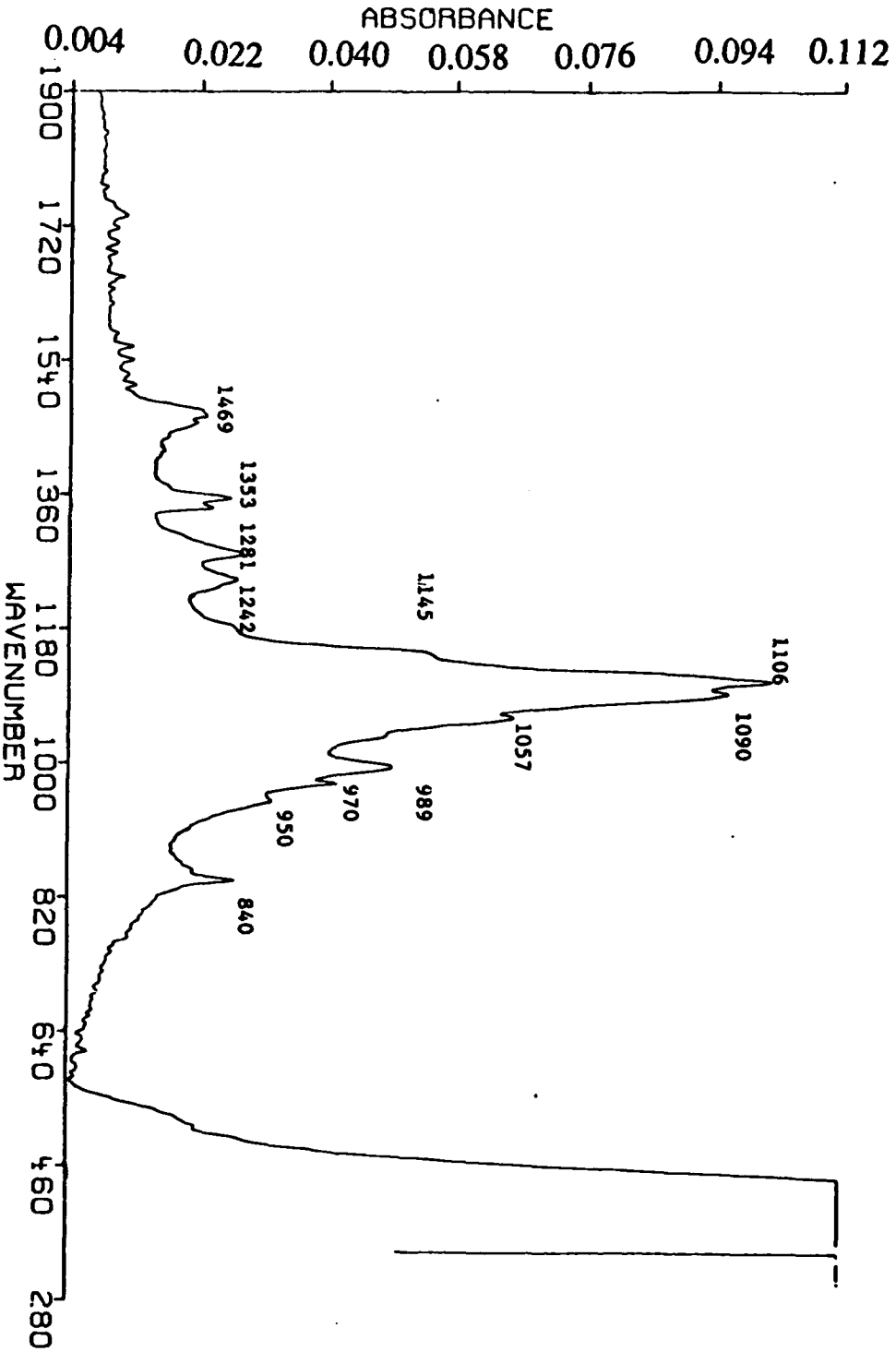

Figure 12. Absorbance Spectrum of a PEO:$LiBF_4$ (O:Li = 6) Complex in 1900-280 cm^{-1} Region.

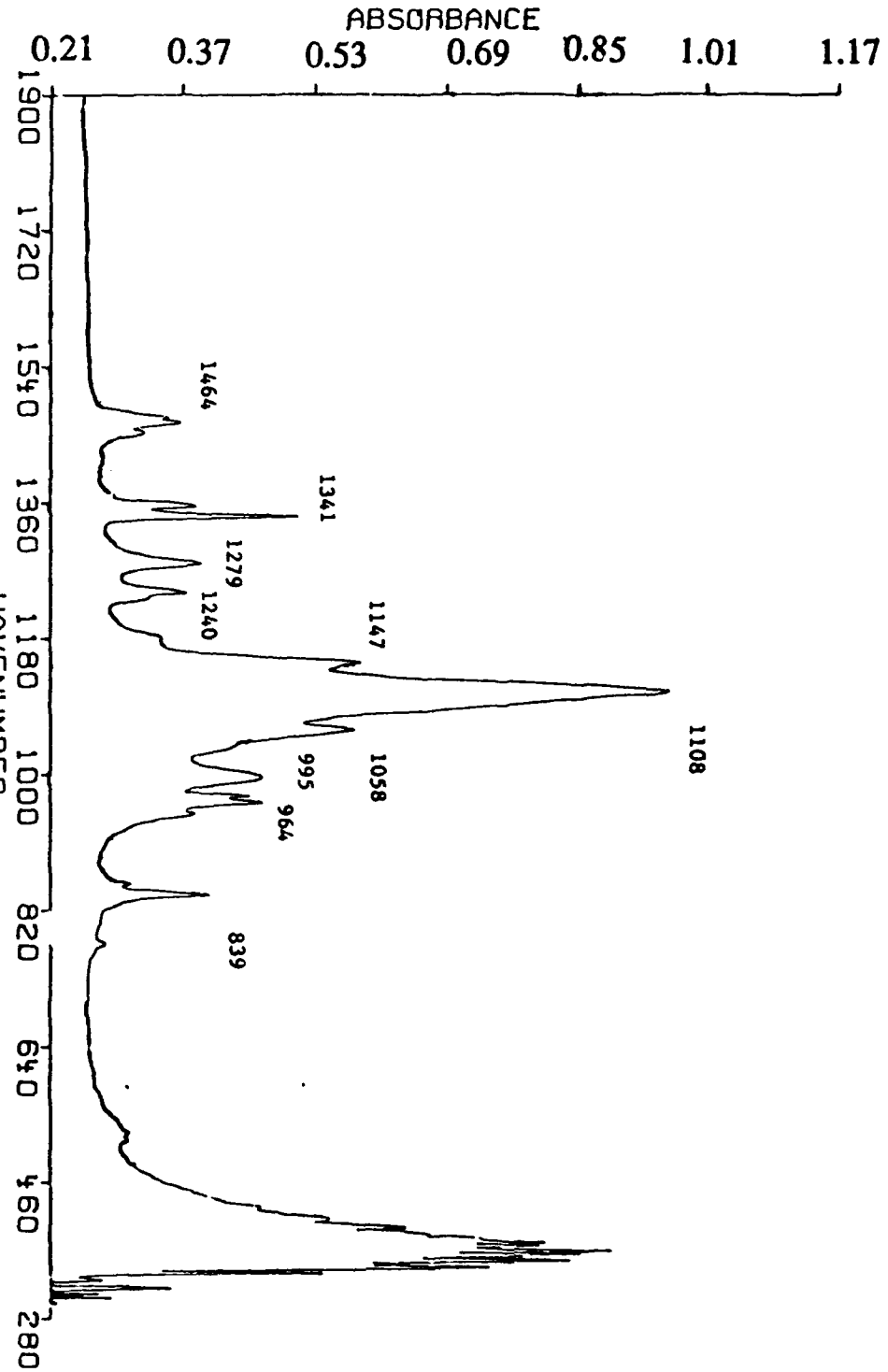

Figure 13. Absorbance Spectrum of a PEO:$LiBF_4$ (O:Li = 8) Complex in 1900-280 cm^{-1} Region.

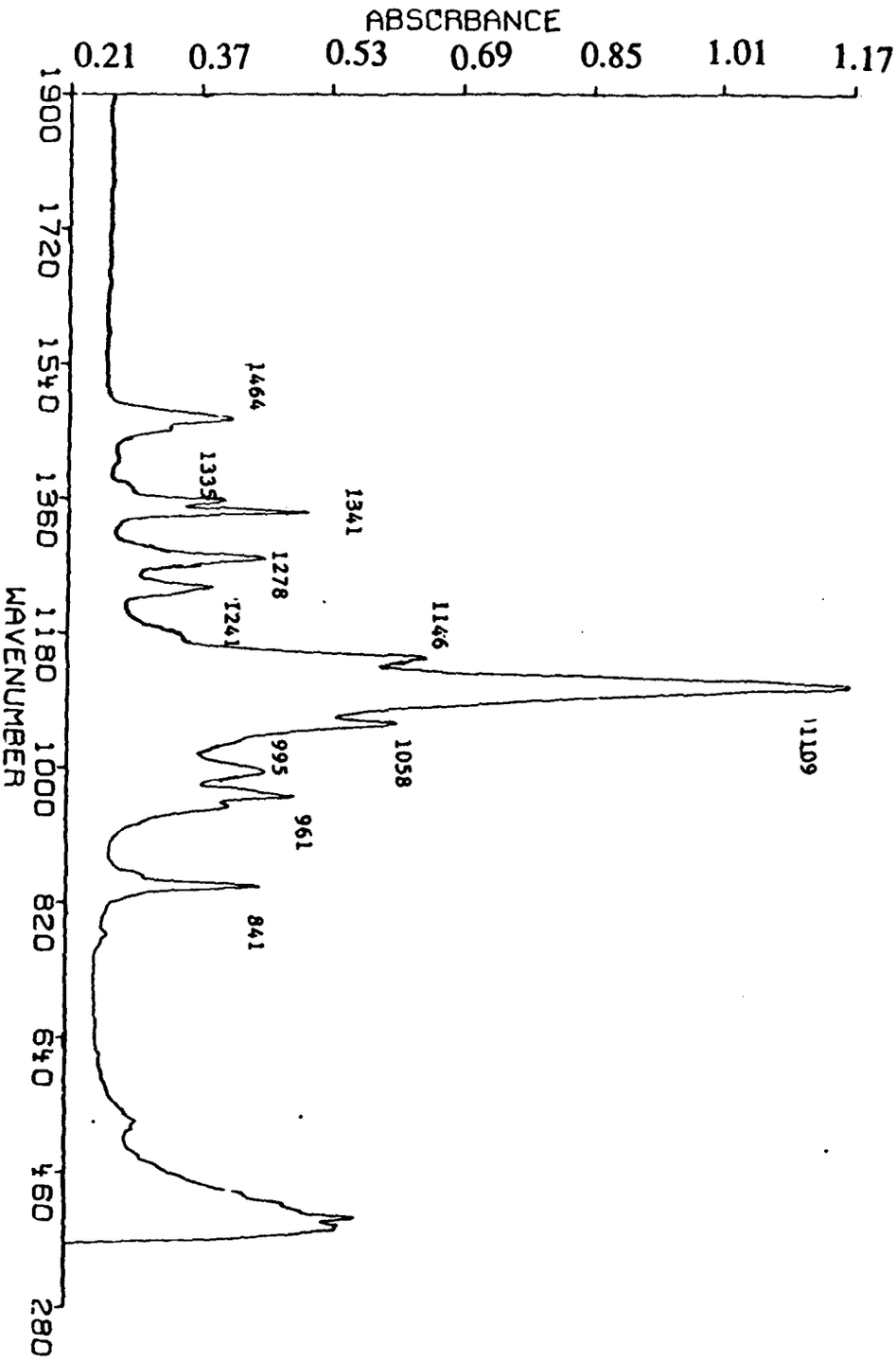

Figure 14. Absorbance Spectrum of a PEO:$LiBF_4$ (O:Li = 10) Complex in 1900-280 cm^{-1} Region.

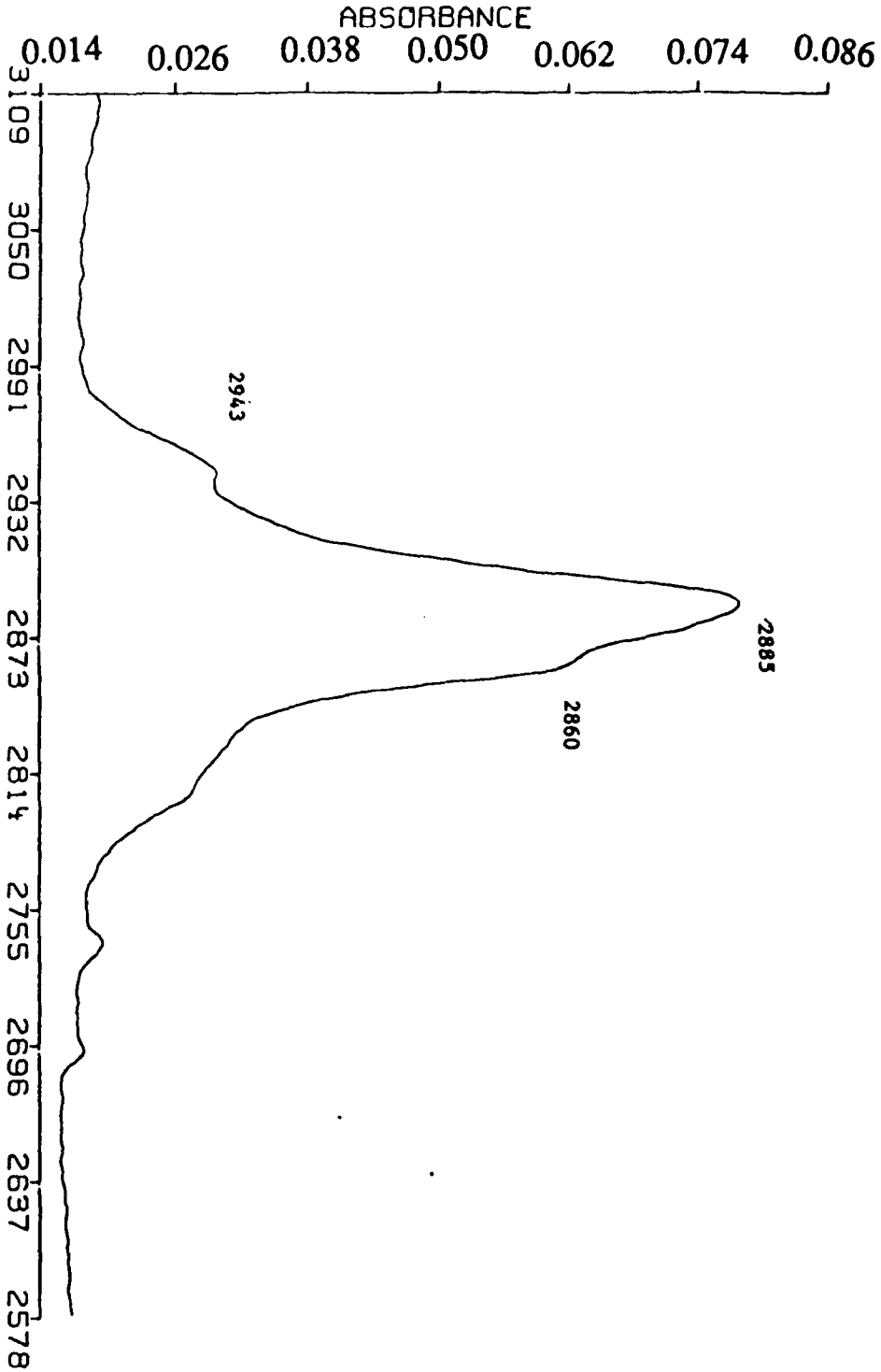

Figure 15. Absorption Spectrum of PEO in 3109-2578 cm^{-1} Region.

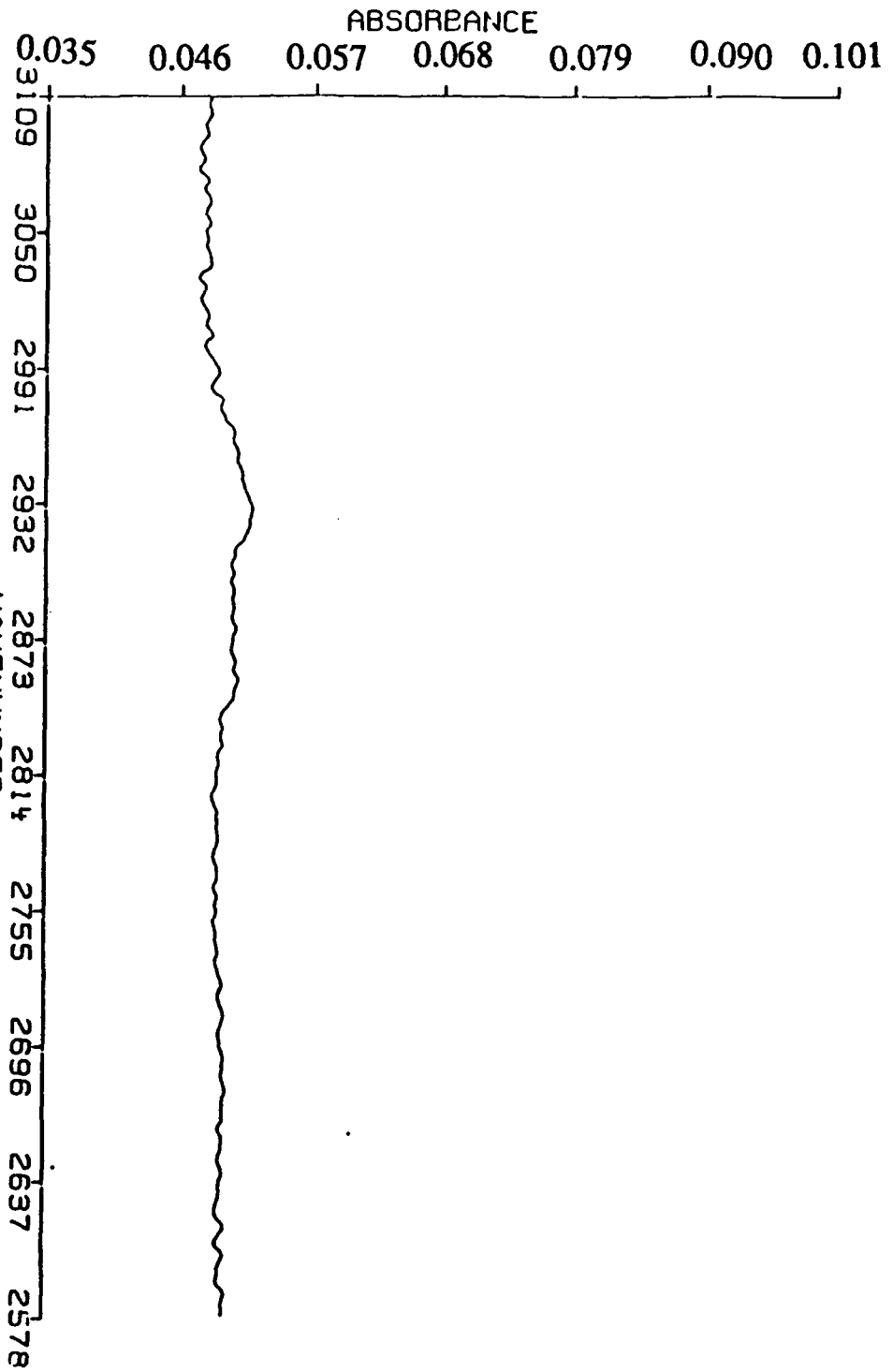

Figure 16. Absorption Spectrum of $LiBF_4$ in 3109-2578 cm^{-1} Region.

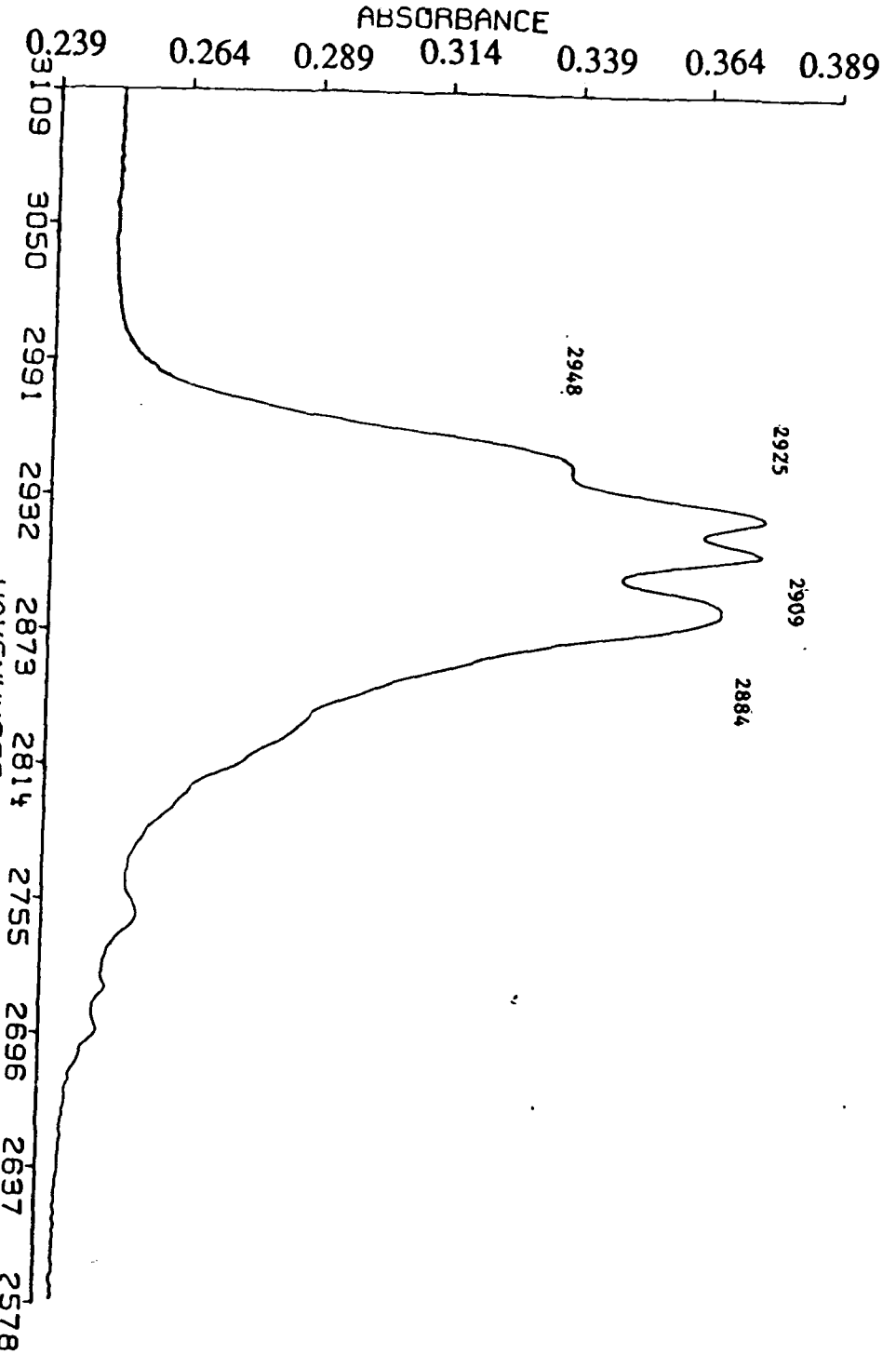

Figure 17. Absorption Spectrum of a TEO:$LiBF_4$ Complex with O:Li Ratio of 3 in 3109-2578 cm^{-1} Region.

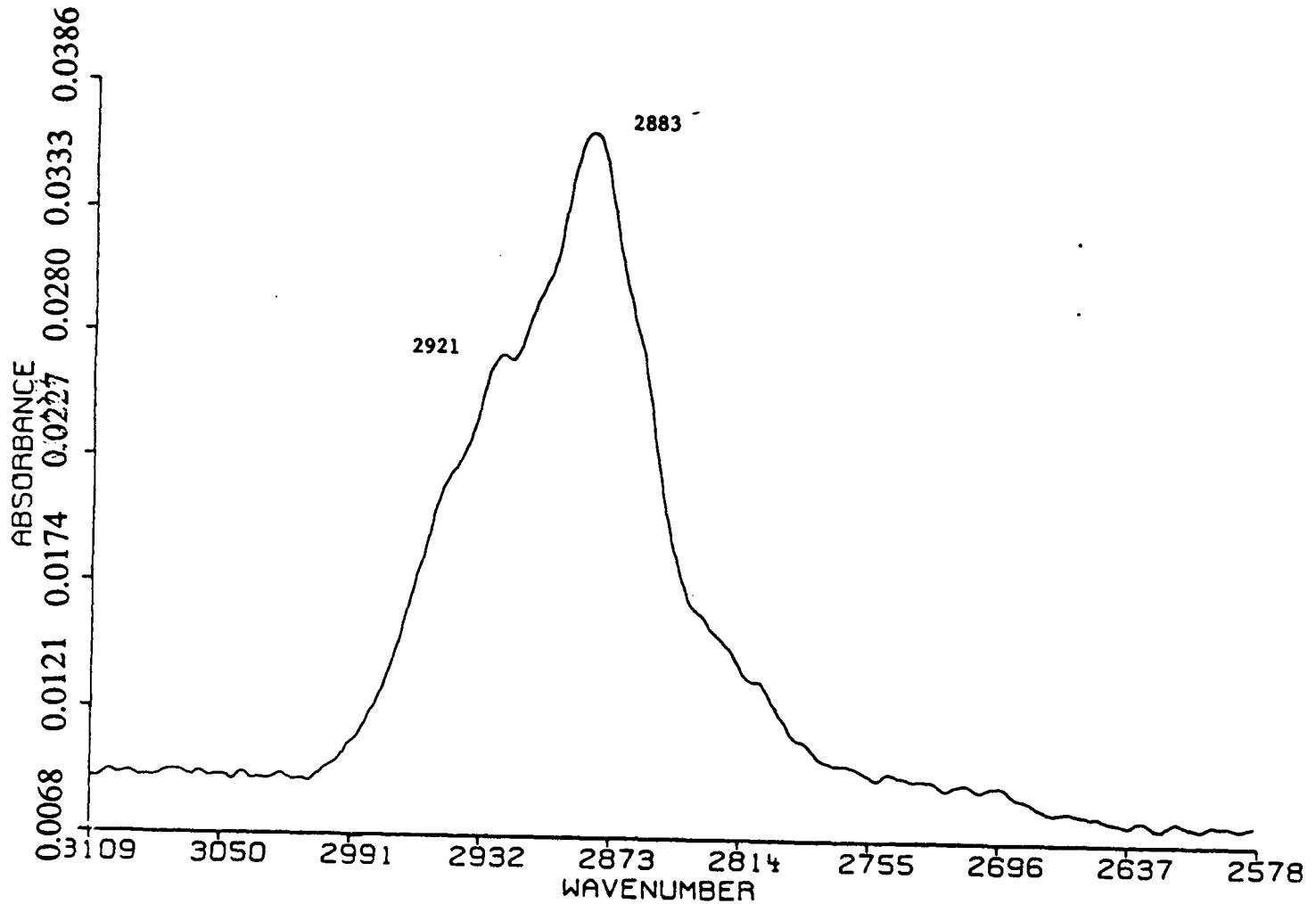

Figure 18. Absorption Spectrum of a PEO:$LiBF_4$ Complex with O:Li Ratio of 6 in 3109-2578 cm^{-1} Region.

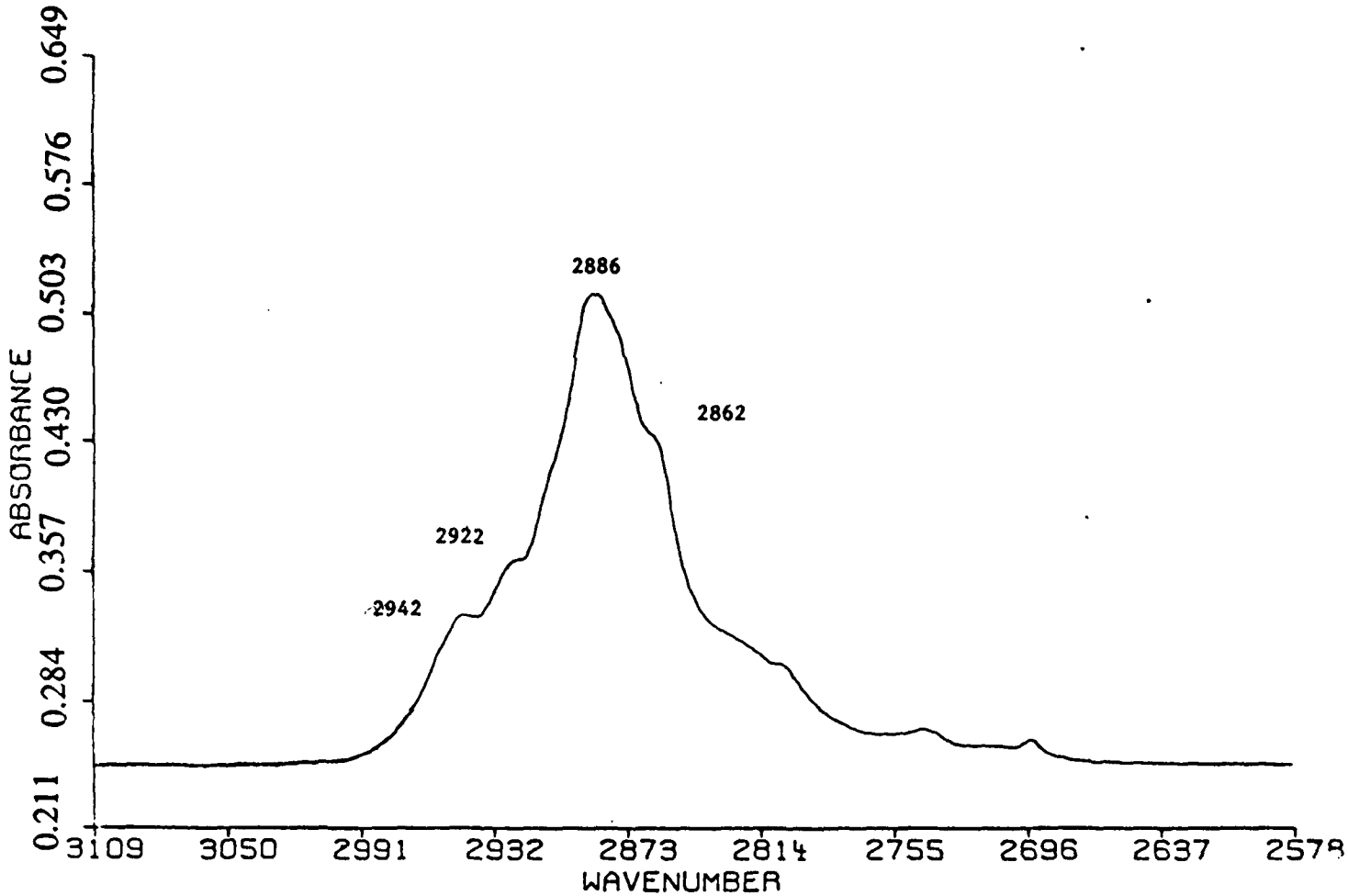

Figure 19. Absorption Spectrum of a PEO:$LiBF_4$ Complex with O:Li Ratio of 8 in 3109-2578 cm^{-1} Region.

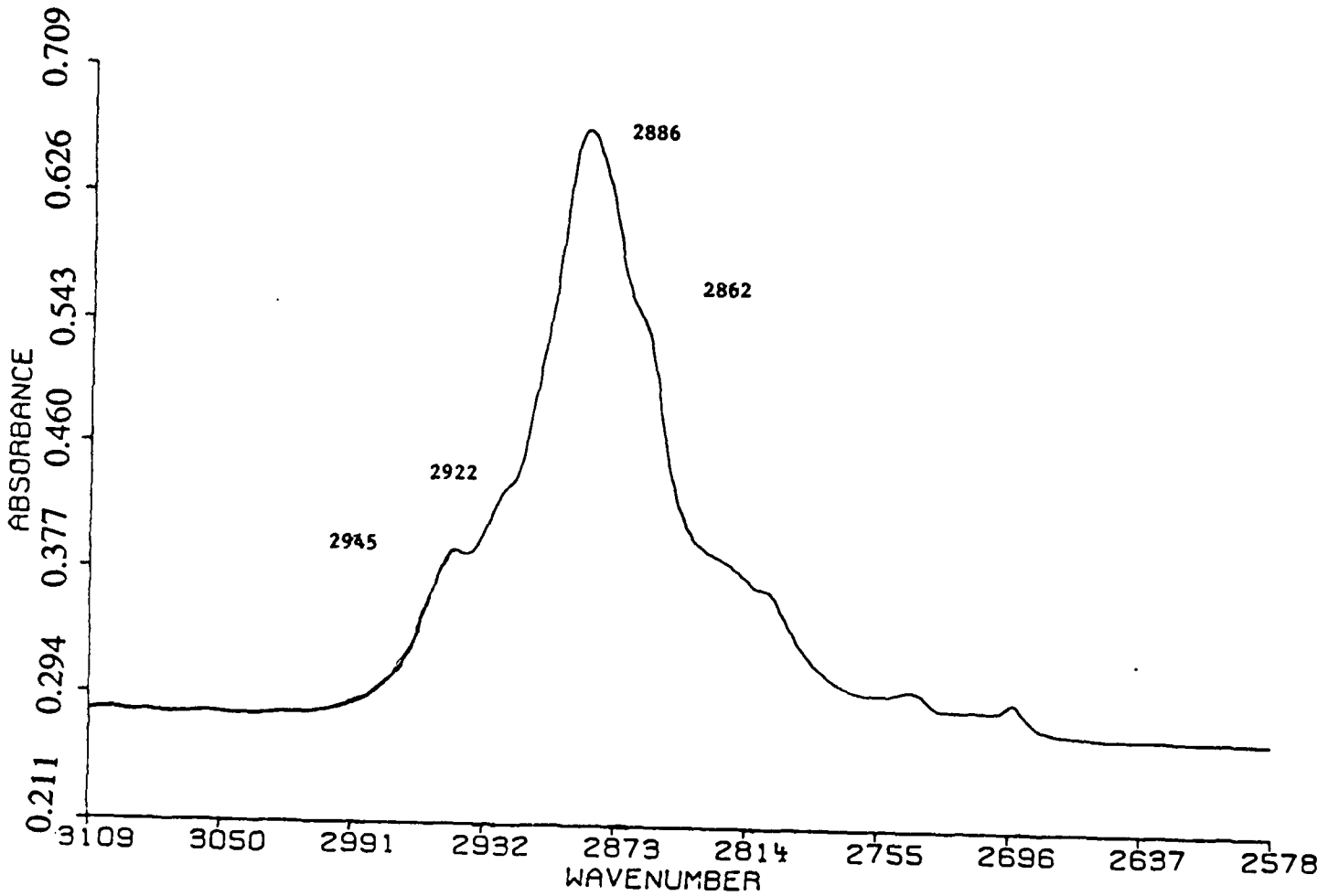

Figure 20. Absorption Spectrum of a PEO:$LiBF_4$ Complex with O:Li Ratio of 10 in 3109-2578 cm^{-1} Region.

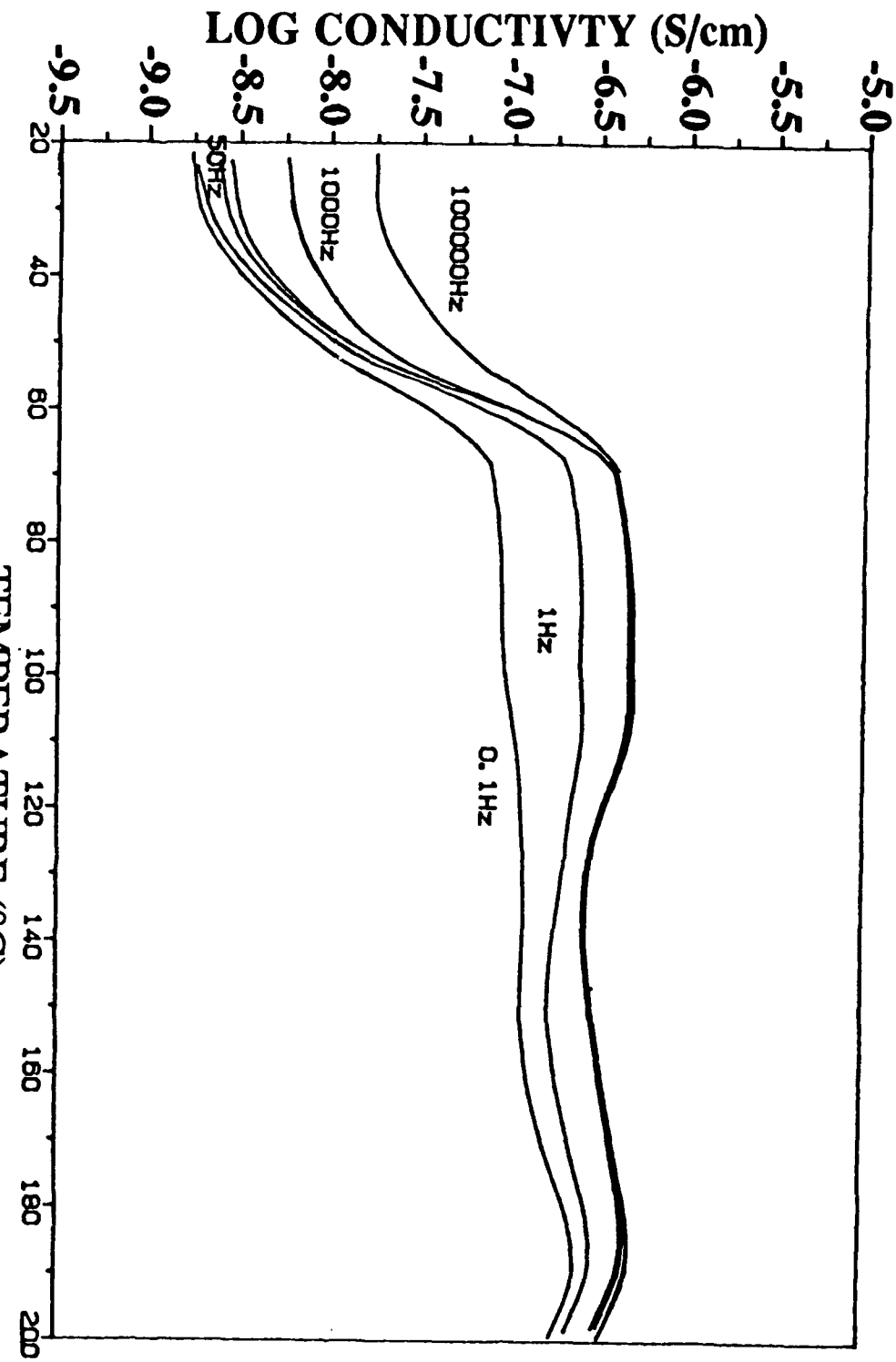

Figure 21. Ionic Conductivity of PEO at Different Frequencies as a Function of Temperature.

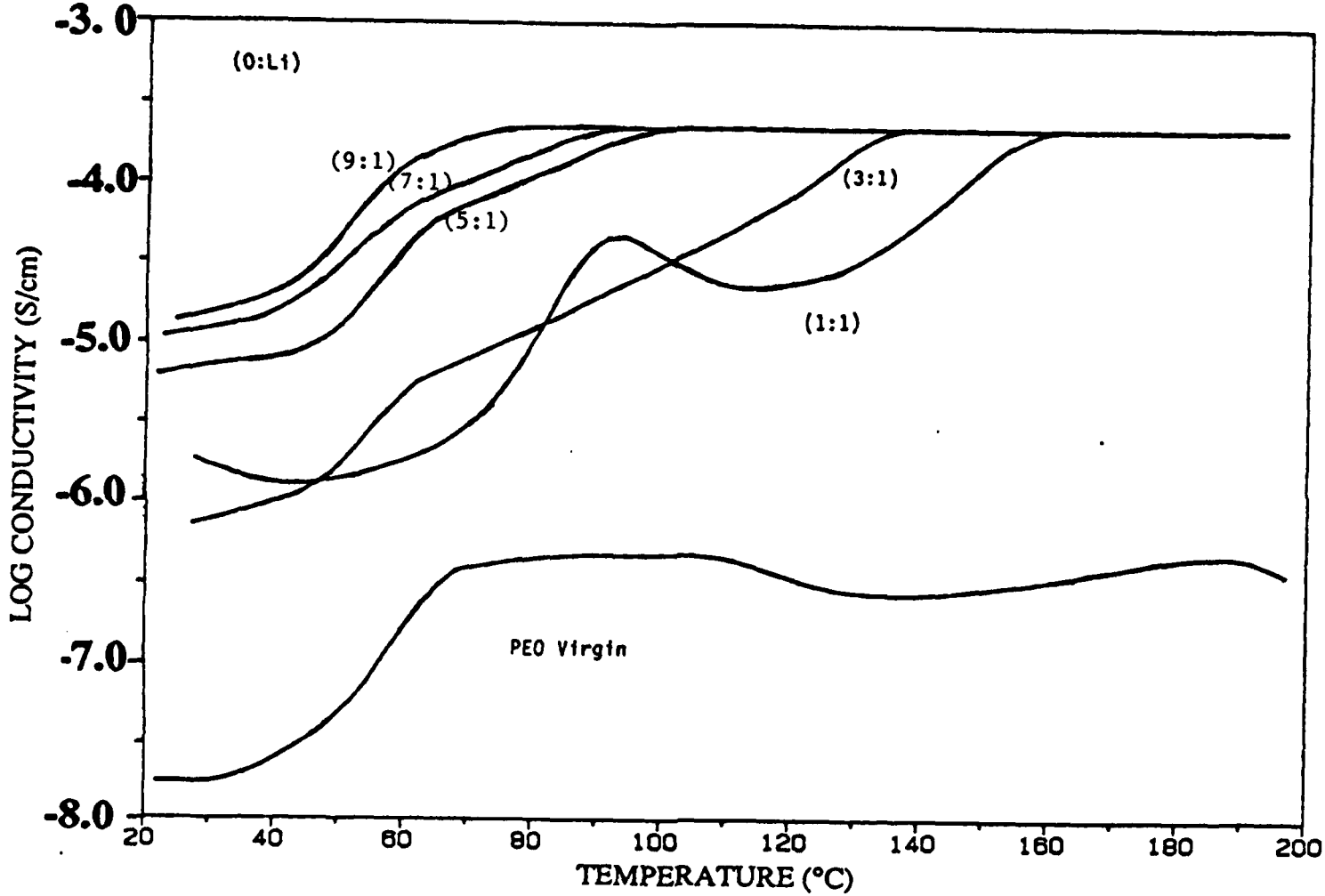

Figure 22. Apparent Ionic Conductivity at Different Dopant Concentration as a Function of Temperature.

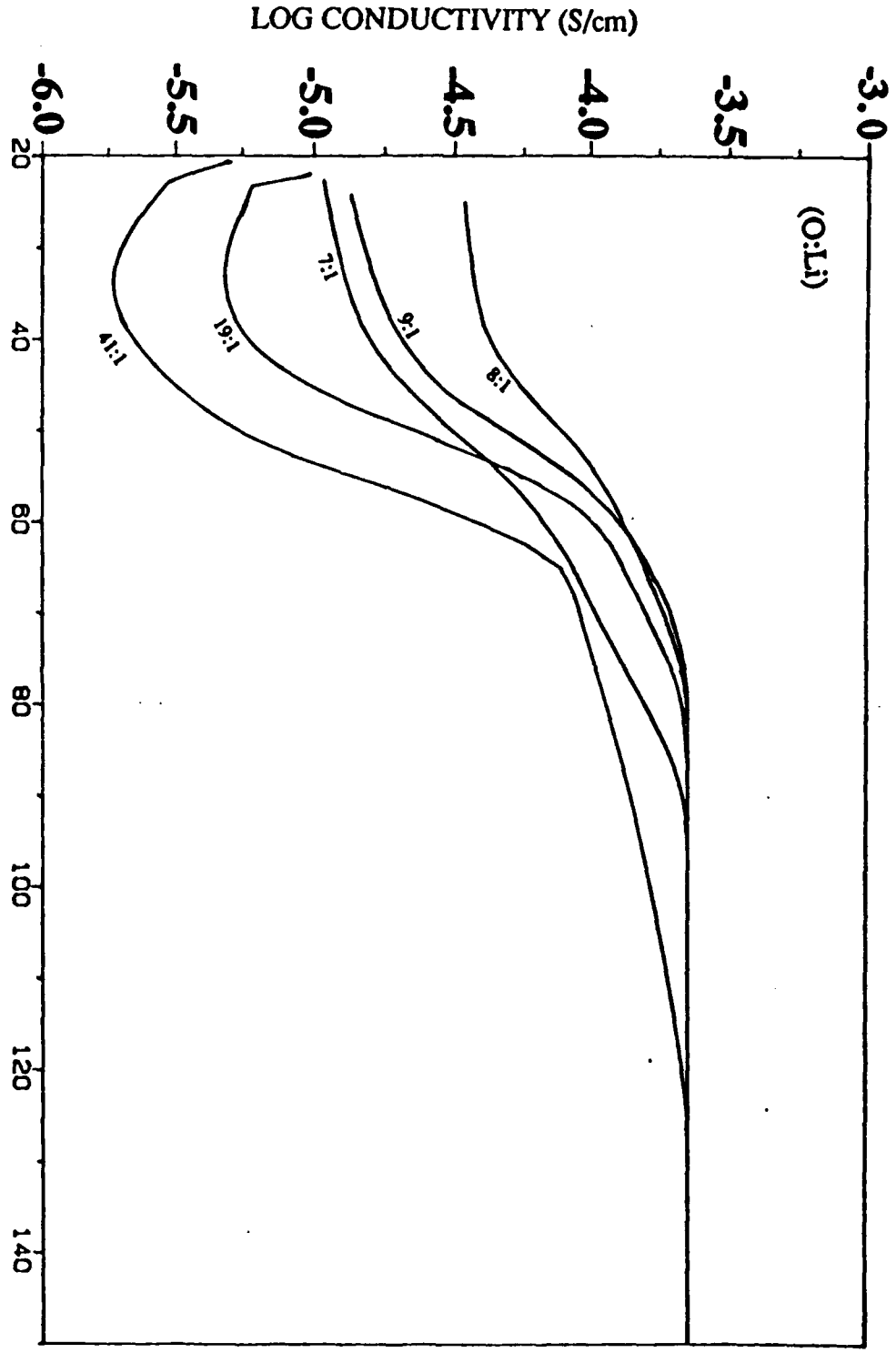

Figure 23. Apparent Ionic Conductivity at Low Dopant Concentration as a Function of Temperature.

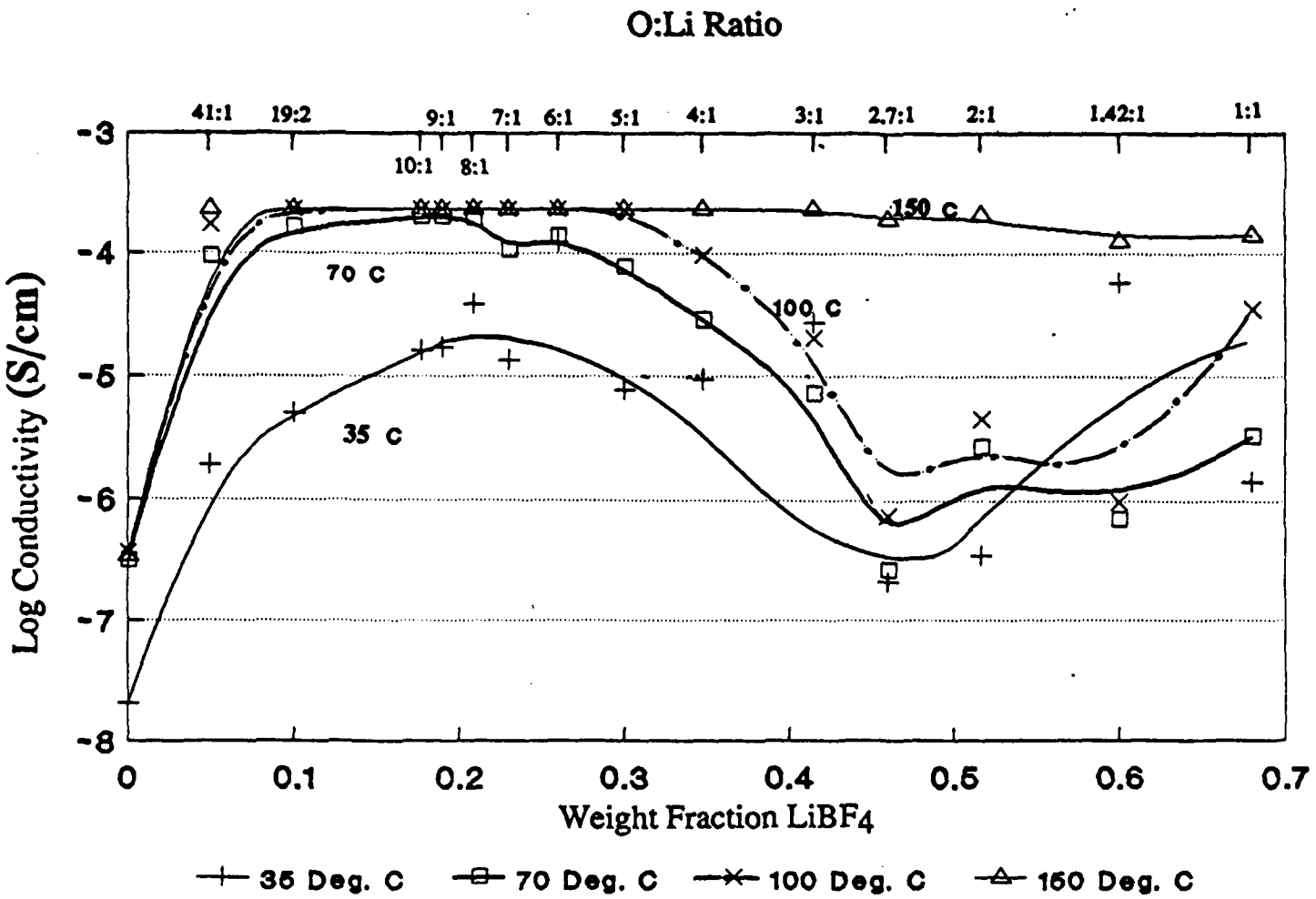

Figure 24. Apparent Ionic Conductivity at Different Temperature as a Function of Weight Fraction of $LiBF_4$.

Figure 25. Dielectric Constant at Different Frequencies as a Function of Temperature.

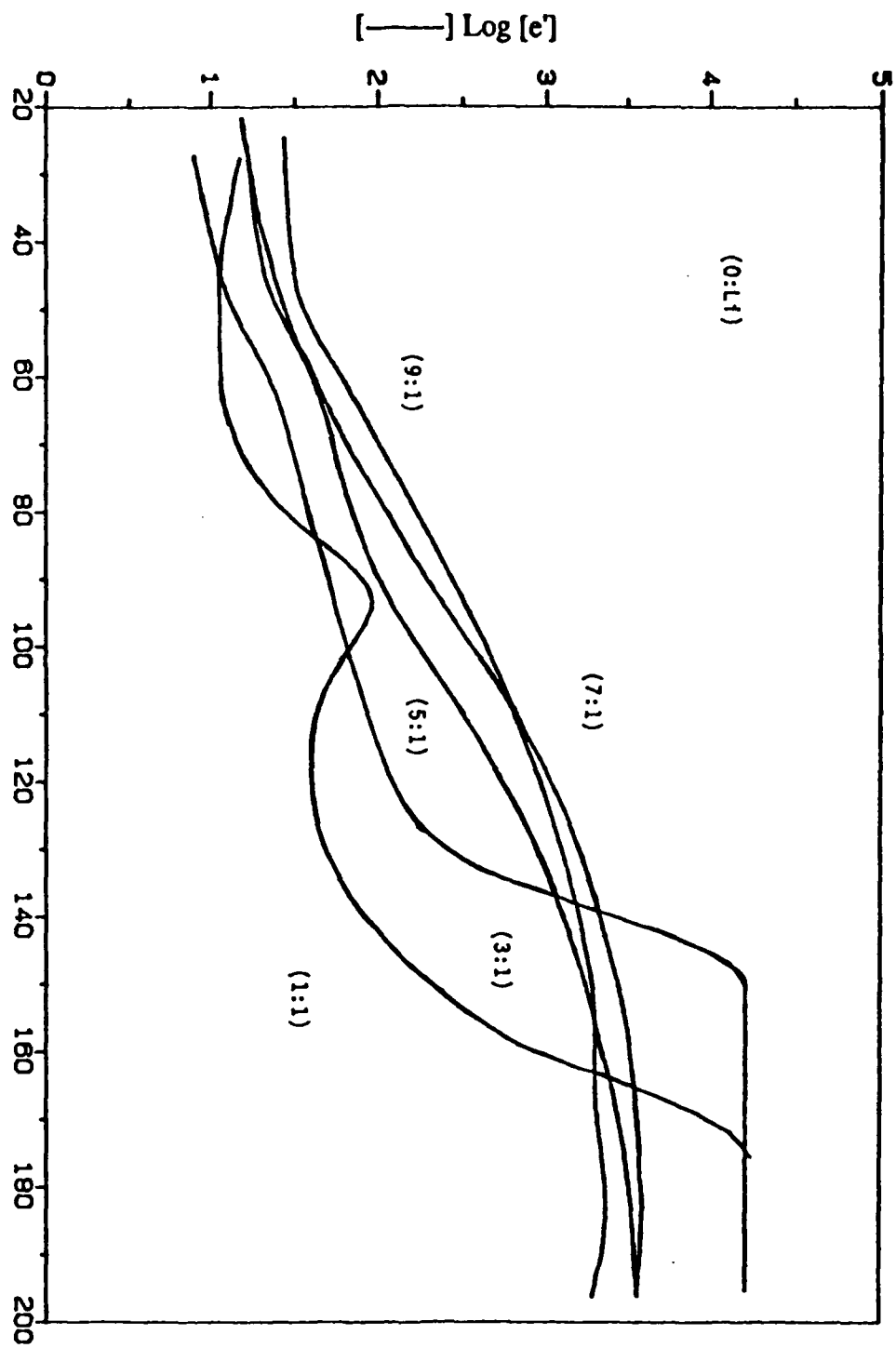

Figure 26. Dielectric Constant at Different $LiBF_4$ Concentration as a Function of Temperature.

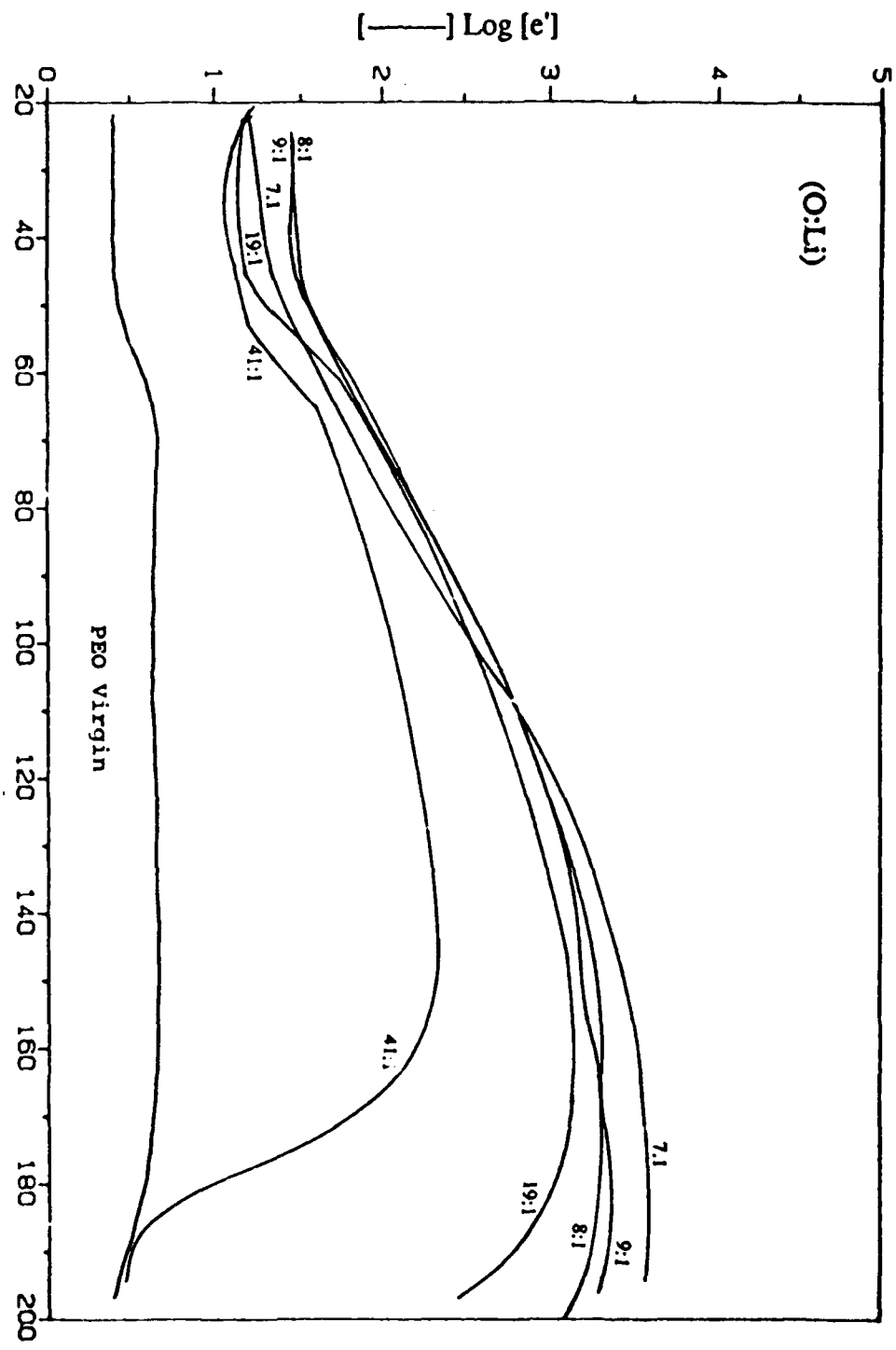

Figure 27. Dielectric Constant at Low $LiBF_4$ Concentration as a Function of Temperature.

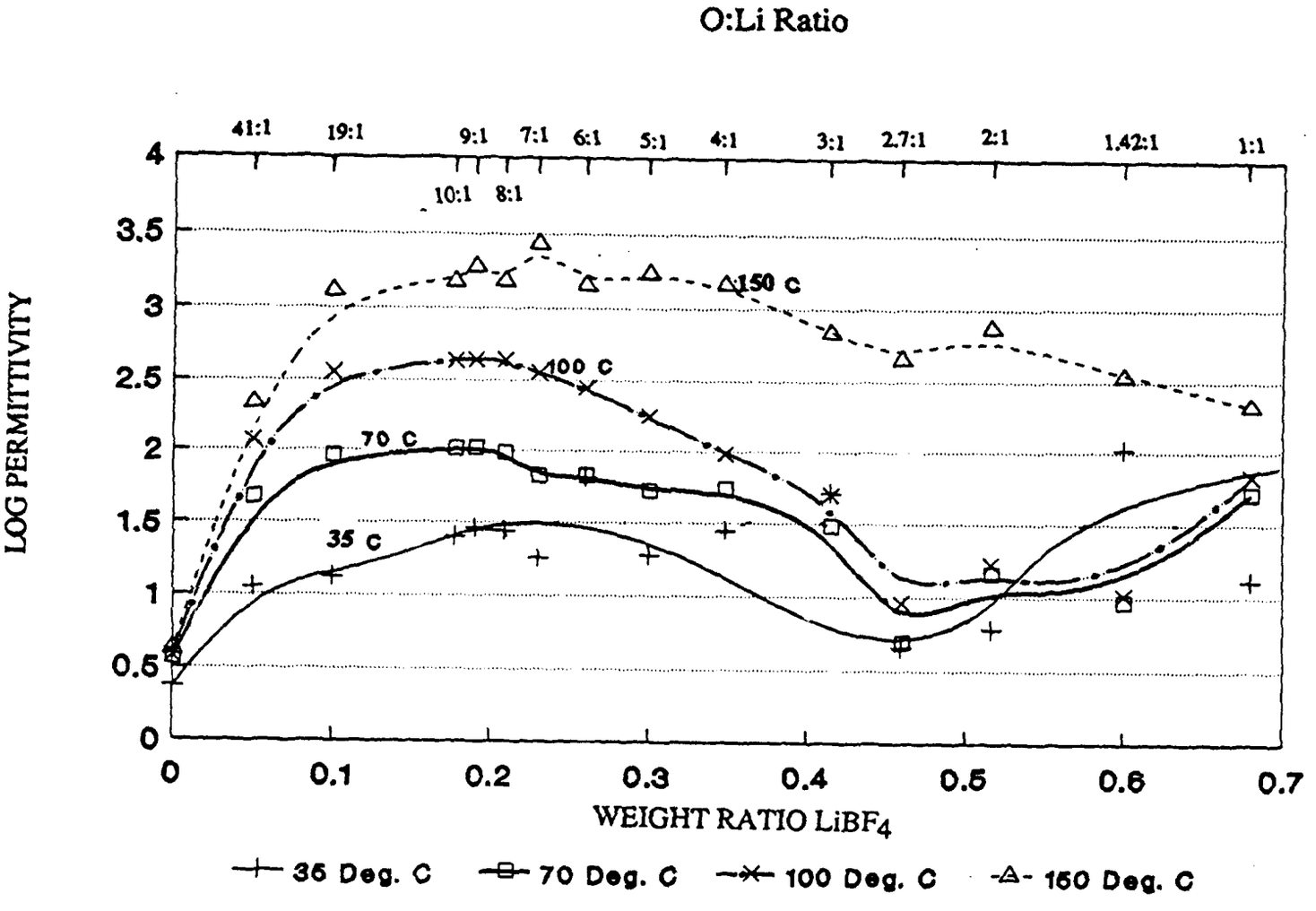

Figure 28. Dielectric Constant at Different Temperature as a Function of Weight Fraction of $LiBF_4$.

Figure 29. Complex Plane Impedance Diagram of a Li/Polymer:$LiBF_4$/Li Cell.

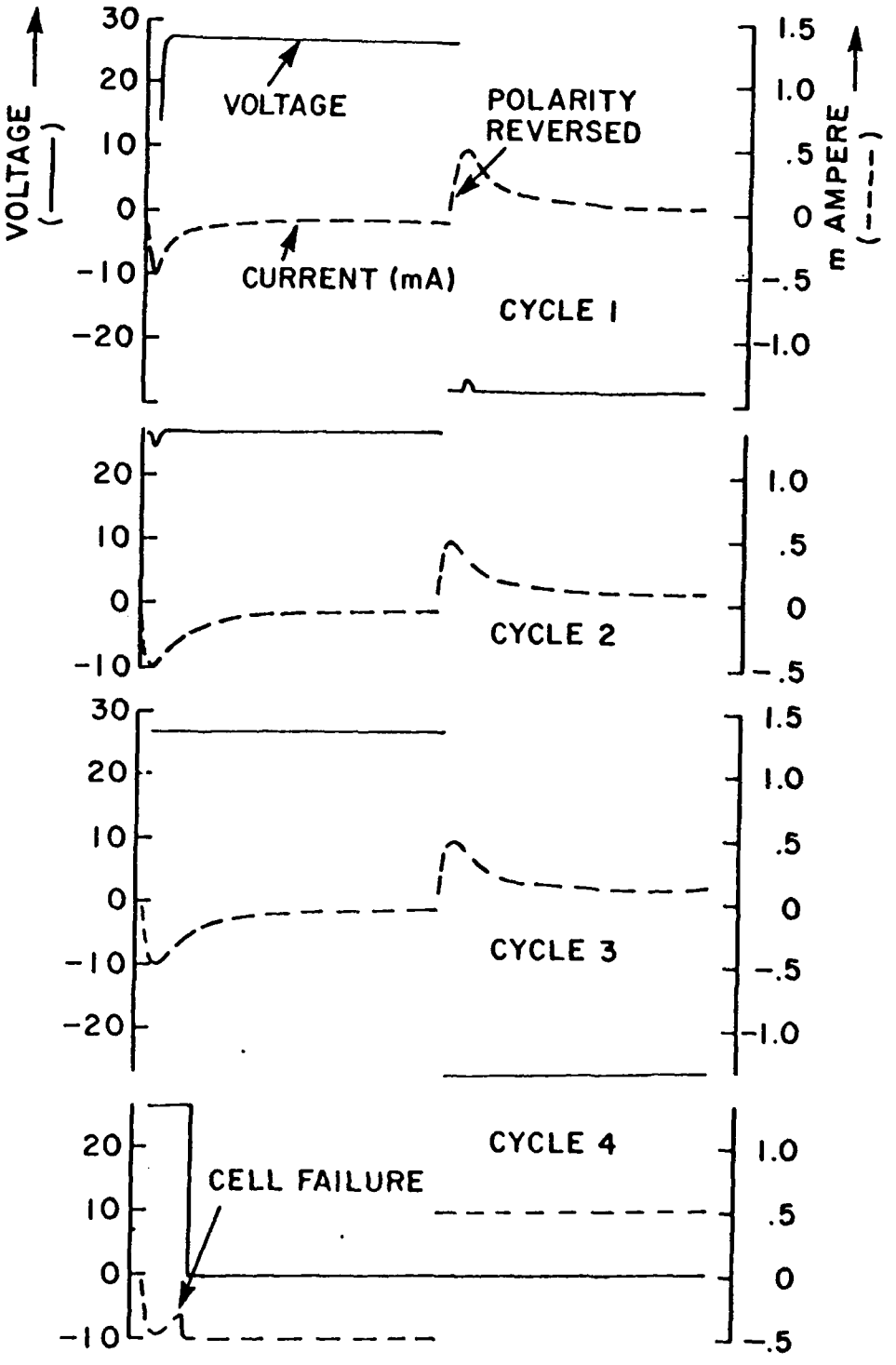

Figure 30. Performance of a Li/PEO:$LiBF_4$/Li Cell Under Cyclic Flow of Current. A Cycle Consisted of a Flow of Current for Two Hours in One Direction Followed by a Reversed Flow for Another Two Hours.

REFERENCES

1. TA Instruments Literature on DEA 2970.

2. Armand, M.B., in "Polymer Electrolyte Reviews-1," J.R. MacCallum and C.A. Vincent, eds., Elsevier Appl. Sci., London and New York, 1987, p. 7.

3. Tonge, J.S. and Shriver, D.F., in "Polymers for Electronic Applications," J.H. Lai, ed. CRC Press, 1989, pp. 185-187.

4. Armand, M.B., Chabagno, J.M., and Duclot, M.J., Second International Meeting on Solid Electrolytes, St. Andrews, Scotland, Sep. 20-22, 1978.

5. Pearson, R.G., J. Chem. Ed. 5, 581 (1968).

6. Shriver, D.F., Papke, B.L., Ratner, M.A., DuPon, R., Wong, T., and Brodwin, M., Solid State Ionics, 5, 83 (1981).

7. Chabagno, J.M.,Ph.D. Thesis, University of Grenoble, 1980; Papke, B.L., Ph.D., Thesis, Northwestern University, 1982.

8. Ratner, M.A., in "Polymer Electrolyte Reviews-1," J.R. MacCallum and C.A. Vincent, eds., Elsevier Appl. Sci., London and New York, 1987, p. 177.

9. Papke, B.L., Ratner, M.A. and Shriver, D.F., J. Electrochem. Soc., 129, 1694 (1982).

10. Bouridah, A., Dalard, F., Deroo, D., Cheradame, H. and LeNest, J.F., Solid State Ionics, 15, 233 (1985).

11. Marcus, Y., Ion Solvation, Wiley, Chichester, 1985.

12. MacCallum, J.R. and Vincent, C.A., "Polymer Electrolyte Reviews-1," Elsevier Applied Science, London and New York, 1987, pp. 24, 32.

13. Fauteux, D., in "Polymer Electrolyte Reviews-1," J.R. MacCallum and C.A. Vincent, Eds., Elsevier Applied Science, London and New York, 1987, p. 121.

14. Minier, M., Berthier, C. and Gorecki, W., Solid State Ionics, 9/10, 1125 (1983).

15. Sorensen, P.R. and Jacobsen, T., Polym. Bull., 9, 47 (1983).

16. Fauteux, D., Lupien, M.D., and Robitaille, C.D., J. Electrochem. Soc., 134, 2761 (1987).

17. Ferloni, P., Chiodelli, G., Magistris, A., and Sanesi, M., Solid State Ionics, 18/19, 265 (1986).

18. Robitaille, C.D. and Fauteux, D., J. Electrochem. Soc., 133, 315 (1986).

19. Hibma, T., Solid State Ionics, 9/10, 1101 (1983).

20. Lee, Y.L. and Crist, B., J. Appl. Phys. 60, 2683 (1986).

21. Minier, M., Berthier, C., and Gorecki, W., J. de Physique 45, 739 (1984).

22. Berthier, C., Gorecki, W., Minier, M., Armand, M.B., Chabagno, J.M., and Rigaud, P., Solid State Ionics, 11, 91 (1983).

23. Zahurak, S.M., Kaplan, M.L., Rietman, E.A., Murphy, D.W. and Cava, R.J., Macromolecules, 21, 654 (1988).

24 Lee, C.C. and Wright, P.V., Polymer, 23, 681 (1982).

25. Fenton, D.E., Parker, J.M. and Wright, P.V., Polymer, 14, 589 (1973).

26. Wright, P.V., British Polym. J., 7, 319 (1975).

27. Payne, D.R. and Wright, P.V., Polymer, 23, 690 (1982).

28. Hibina, T., Solid State Ionics 91, 1101 (1983).

29. Weston, J.E. and Steele, B.C.H., Solid State Ionics, 7, 81 (1982).

30. Weston, J.E. and Steele, B.C.H., Solid State Ionics, 2, 347 (1981).

31. Fauteux, D., Ph.D. Thesis, University of Grenoble, France.

32. Papke, B.L., Ratner, M.A., and Shriver, D.F., J. Electrochem. Soc., 129, 1434 (1982).

33. Halsam, J. and Willis, H.A., "Identification and Analysis of Plastics;" D. Van Nasfrand Co. Inc. London, 1965, pp. 246.

34. Papke, B.L., DuPon, R., Ratner, M.A., and Shriver, D.F., Solid State Ionics 5, 685 (1981).

35. Torell, L.M. and Schantz, S. in "Polymer Electrolyte Review-2," MacCallum, J.R. and Vincent, C.A., eds., Elsevier Applied Science, London and New York, Ch. 1, 1989.

36. Greenbaum, S.G., Pak, Y.S., Wintersgill, M.C., Fontanella, J.J., Schultz, J.W., and Andeen, C.G., J. Electrochem. Soc., 135, 235 (1988).

37. Wintersgill, M.C., Fontanella, J.J., Greenbaum, S.G., and Adamic', K.J., Br. Poly. J., 20, 195 (1988).

38. Gorecki, W., Thesis, University of Grenoble, 1984.

39. Porter, C.H. and Boyd, R.H., Macromolecules, 4, 589 (1971).

40. Wintersgill, M.C. and Fontanella, J.J., in "Polymer Electrolyte Reviews-2," MacCallum, J.R. and Vincent, C.A., eds., Elsevier Applied Science, London, pg. 46, 1989.

 ☆U.S. GOVERNMENT PRINTING OFFICE: 1992 - 648-127/62276